รายงานวิจัยฉบับสมบูรณ์

โครงการ

Structure, Sorption and Reaction Dynamics in Catalytic Systems

โดย

จำรัส ลิ้มตระกูล

1 ธันวาคม 2544

รายงานวิจัยฉบับสมบูรณ์

โครงการ

Structure, Sorption and Reaction Dynamics in Catalytic Systems

โดย

จำรัส ลิ้มตระกูล

1 ธันวาคม 2544

สำนักงานกองทุนสนับสนุนการวิจัย (สกว.)
ชั้น 14 อาคาร เอส เอ็ม ทาวเวอร์
เลขที่ 979/17-21 ถนนพหลโยธิน แขวงสามเสนใน
เขตพญาไท กรุงเทพฯ 10400
โทร.298-0455 โทรสาร 298-0476
Home page : http://www.trf.or.th
E-mail : trf-info@trf.or.th

สัญญาเลขที่ RSA/01/2541

รายงานวิจัยฉบับสมบูรณ์

โครงการ

Structure, Sorption and Reaction Dynamics in Catalytic Systems

โดย

จำรัส ลิ้มตระกูล

ภาควิชาเคมี คณะวิทยาศาสตร์

มหาวิทยาลัยเกษตรศาสตร์

สนับสนุนโดยสำนักงานกองทุนสนับสนุนการวิจัย

(ความเห็นในรายงานนี้เป็นของผู้วิจัย สกว. ไม่จำเป็นต้องเห็นด้วยเสมอไป)

Acknowledgements

J. P. thanks the Thailand Research Fund for financial support. We are also grateful to the Utah supercomputer for allowance of computational researches.

Special thanks go to Piti Treesukol, Parawan Chuichai, Pipat Kongpracha Somkiat Nokbin, Siriporn Jungsuttiwong, and Tanin Nanok who did a lot of calculations.

J.P. is also grateful to many colleagues of the Laboratory for Computational and Applied Chemistry.

รหัสโครงการ: RSA/01/2541

ชื่อโครงการ: Structure, Sorption and Reaction Dynamics in Catalytic Systems

ชื่อนักวิจัย: จำรัส ลิ้มตระกูล
E-mail Address: fscijrl@ku.ac.th

ระยะเวลาโครงการ: 3 ปี

วัตถุประสงค์

เพื่อที่จะพัฒนาระเบียบวิธีการศึกษาตำแหน่งของการเกิดปฏิกิริยา การดูดซับ และการเกิดปฏิกิริยาของตัวเร่งปฏิกิริยาที่มีโครงสร้างในระดับนาโน

ระเบียบวิธีการศึกษาวิจัย

เนื่องจากการสร้างแบบจำลองปฏิกิริยาบนตัวเร่งปฏิกิริยาเป็นเรื่องที่ท้าทายในเชิงทฤษฎี ดังนั้นเราจึงมุ่งเน้นที่จะทำการออกแบบโครงสร้าง การดูดซับ และทำการศึกษาการเกิดปฏิกิริยาในระบบที่มีตัวเร่งโดยใช้ระเบียบวิธี Electronic structure cluster และ Electronic embedded cluster สำหรับระเบียบวิธี Electronic embedded cluster นี้คือการฝัง Reactive cluster ลงในสนามศักย์ที่เกิดจากโครงสร้างทั้งหมดของซีโอไลต์ (lattice framework) ซึ่งจะเป็นการเพิ่มความถูกต้องให้กับแบบจำลองและสามารถนำไปใช้ในการทำนายกลไกของการเกิดปฏิกิริยาได้อย่างมีประสิทธิภาพ

ผลการทดลอง

การออกแบบจำลองโครงสร้างของตัวเร่งปฏิกิริยาซีโอไลต์ชนิด ZSM-5 ทำได้โดยการจำลองจากโครงสร้างจริงของ ZSM-5 และทำการแทนที่ Si ที่ตำแหน่ง T12 ด้วย Al เพื่อที่จะทำให้เกิด Lewis base ซึ่งเป็น active site แล้วทำการดุลประจุลบที่เกิดจาก $[AlO4]^-$ ด้วย Cu(I), Ag(I), Li(I) หรือ H^+

ในการศึกษานี้เลือกใช้แบบจำลอง Cluster ทั้งหมด 4 ชนิดที่มีขนาดตั้งแต่ 3T ถึง 10T เมื่อ T คือ tetrahedral ของ Si หรือ Al ($SiO4$ หรือ $AlO4^-$) ที่ตัดมาจากโครงสร้างของ ZSM-5

การนำ Quantum cluster ฝังลงในสนามศักย์ของ point charges ซึ่งสร้างจากเทคนิควิธี SCREEP นั้นก็เพื่อเพิ่มความถูกต้องให้กับแบบจำลอง โดยเทคนิคนี้เป็นการรวมเอาผลจากสิ่งแวดล้อมในโครงสร้างจริงของซีโอไลต์ที่ได้ตัดทิ้งไปเข้ามาด้วย

สรุปและวิจารณ์ผล

การออกแบบตัวเร่งปฏิกิริยาในระดับนาโนถือว่าเป็นหัวข้อการวิจัยทางเคมีที่น่าสนใจ และเป็นที่ทราบกันดีว่าซีโอไลต์เป็นตัวเร่งปฏิกิริยาที่สำคัญในอุตสาหกรรมเคมี คุณสมบัติทางกายภาพและทางเคมีที่สำคัญของตัวเร่งเหล่านี้ขึ้นอยู่กับโครงสร้างของ framework ที่ล้อมรอบโลหะ ตัวเร่งเหล่านี้สามารถปรับปรุงด้วยวิธีการที่เหมาะสมเพื่อให้ได้ผลิตภัณฑ์หรือโมเลกุลเป้าหมายสูงสุด ทั้งนี้เราได้ทำการศึกษาปัญหาที่น่าสนใจของระบบตัวเร่งปฏิกิริยาในระดับนาโนหลายหัวข้อ เช่น การดูดซับ ตำแหน่งของโปรตอน และปฏิกิริยาของสารประกอบไฮโดรคาร์บอน

คำหลัก: zeolite, embedded cluster, adsorption, catalysts.

Project Code: RSA/01/2541
Project Title: Structure, Sorption and Reaction dynamics in Catalytic Systems
Investigator: Jumras Limtrakul
E-mail Address: fscijrl@ku.ac.th
Project Period: 3 years

Objectives

Our aim is to develop strategies for investigating reactive center, adsorption, and reaction dynamics in nanostructured catalysts.

Research Methodologies

Modeling reactivity of catalysts has been a theoretical challenge. Our focus has been to design structure, sorption and reaction dynamics in catalytic systems using Electronic Structure Cluster and Electronic Embedded Cluster methods. In this new electronic embedded cluster methodology, the active site is modeled as a reactive cluster embedded in a long-range electrostatic effect of the zeolitic crystal. This allows the active site to be carried out at an accurate level of electronic structure theory while the influences of zeolite crystal are effectively included. Combining this with the conventional cluster method will provide us a powerful tool to predict reaction mechanisms in catalysts.

Results and Discussion

The ZSM-5 structure was taken from the silicious ZSM-5 crystal To represent the Lewis basic active site, the silicon atom of the T12 site was substituted by an aluminum atom. An Cu(I), Ag(I), Li(I) and H^+ ion were added to counterbalance the negative charge of [AlO4]-.

Four clusters ranging from 3T to 10T, where T is Si- or Al tetrahedral (SiO4 or $AlO4^-$), were cut from the ZSM-5 lattice. Due to the partial covalent nature of zeolite, the boundary Si atoms of each cluster were saturated by capped hydrogen atoms located along the broken Si-O bonds in ZSM-5 lattice with an Si-H bond distance of 1.47 Å. The boundary SiH3 groups were held fixed in all geometry optimizations.

To incorporate the environmental effects of the remaining zeolite framework, the QM clusters are embedded in a potential field of point charges. The SCREEP method was used to construct these point charges. To account for the electrostatic potential from the capped hydrogen atoms and to minimize their interactions with the external point charges, we removed the first shell of external charges closest to the QM cluster and adjusted the charge's values of the next shell to reproduce the correct classical Madelung potential calculated from the Ewald-sum method in the active site region.

Nonlocal hybrid density functional theory, particularly the B3LYP functional, was used in this study due to its consistency and reliability in zeolite systems.

Conclusion

Rational catalyst design, notably nanostructured materials, represents one of the most rewarding challenges in chemical research. Zeolites have been used as catalysts in many industrial processes, in addition to many other uses due to their nanostructured framework. They play a significant role in chemicals and fuels production. Their physicochemical properties are based on the ability of the open framework structures to enclose metals [Fe, Cu Ag, Pt, etc.], charged and neutral species as well as nanocluster with in cavities. These nonstructural catalysts can be tailored or tuned to maximize the product of target molecules by employing state-of-the-art techniques. Several interesting problems, namely adsorption, proton sitting, and reactions of hydrocarbon in nanostructured catalysts been investigated.

Keyword: zeolite, embedded cluster, adsorption, catalysis.

รหัสโครงการ: RSA/01/2541

ชื่อโครงการ: Structure, Sorption and Reaction dynamics in Catalytic Systems

ชื่อนักวิจัย: จำรัส ลิ้มตระกูล
E-mail Address: fscijrl@ku.ac.th

ระยะเวลาโครงการ: 3 ปี

วัตถุประสงค์

เพื่อที่จะพัฒนาระเบียบวิธีการศึกษาตำแหน่งของการเกิดปฏิกิริยา การดูดซับ และการเกิดปฏิกิริยาในตัวเร่งปฏิกิริยาที่มีโครงสร้างในระดับนาโน

ระเบียบวิธีการศึกษาวิจัย

เนื่องจากการสร้างแบบจำลองปฏิกิริยาบนตัวเร่งปฏิกิริยาเป็นเรื่องที่ท้าทายในเชิงทฤษฎี ดังนั้นเราจึงมุ่งเน้นที่จะทำการออกแบบโครงสร้าง การดูดซับ และทำการศึกษาการเกิดปฏิกิริยาในระบบที่มีตัวเร่งโดยใช้ระเบียบวิธี Electronic structure cluster และ Electronic embedded cluster สำหรับระเบียบวิธี Electronic embedded cluster นี้คือการฝัง Reactive cluster ลงในสนามศักย์ที่เกิดจากโครงสร้างทั้งหมดของซีโอไลต์ (lattice framework) ซึ่งจะเป็นการเพิ่มความถูกต้องให้กับแบบจำลองในทฤษฎีและสามารถนำไปใช้ในการทำนายกลไกของการเกิดปฏิกิริยาได้อย่างมีประสิทธิภาพ

ผลการทดลอง

การออกแบบจำลองโครงสร้างของตัวเร่งปฏิกิริยาซีโอไลต์ชนิด ZSM-5 ทำได้โดยการจำลองจากโครงสร้างจริงของ ZSM-5 และทำการแทนที่ Si ที่ตำแหน่ง T12 ด้วย Al เพื่อที่จะทำให้เกิด Lewis base ซึ่งเป็น active site แล้วทำการดุลประจุลบที่เกิดจาก $[AlO4]^-$ ด้วย Cu(I), Ag(I), Li(I) หรือ H^+

ในการศึกษานี้เลือกใช้แบบจำลอง Cluster ทั้งหมด 4 ชนิดที่มีขนาดตั้งแต่ 3T ถึง 10T เมื่อ T คือ tetrahedral ของ Si หรือ Al ($SiO4$ หรือ $AlO4^-$) ที่ตัดมาจากโครงสร้างของ ZSM-5

การนำ Quantum cluster ฝังลงในสนามศักย์ของ point charges ซึ่งสร้างจากเทคนิควิธี SCREEP นั้นก็เพื่อเพิ่มความถูกต้องให้กับแบบจำลอง โดยเทคนิคนี้เป็นการรวมเอาผลจากสิ่งแวดล้อมในโครงสร้างจริงของซีโอไลต์ที่ได้ตัดทิ้งไปเข้ามาด้วย

สรุปและวิจารณ์ผล

การออกแบบตัวเร่งปฏิกิริยาในระดับนาโนถือว่าเป็นหัวข้อการวิจัยทางเคมีที่น่าสนใจ และเป็นที่ทราบกันดีว่าซีโอไลต์เป็นตัวเร่งปฏิกิริยาที่สำคัญในอุตสาหกรรมเคมี คุณสมบัติทางกายภาพและทางเคมีที่สำคัญของตัวเร่งเหล่านี้ขึ้นอยู่กับโครงสร้างของ framework ที่ล้อมรอบโลหะ ตัวเร่งเหล่านี้สามารถปรับปรุงด้วยวิธีการที่เหมาะสมเพื่อให้ได้ผลิตภัณฑ์หรือโมเลกุลเป้าหมายสูงสุด ทั้งนี้เราได้ทำการศึกษาปัญหาที่น่าสนใจของระบบตัวเร่งปฏิกิริยาในระดับนาโนหลายหัวข้อ เช่น การดูดซับ ตำแหน่งของโปรตอน และปฏิกิริยาของสารประกอบไฮโดรคาร์บอน

คำหลัก: zeolite, embedded cluster, adsorption, catalysts.

TRF Research Scholar (1999-2001)

Structure, Sorption and Reaction Dynamics in Catalytic Systems

Jumras Limtrakul
Physical Chemistry Division, Faculty of Science, Kasetsart University
Bangkok 10900/ THAILAND

Contents

I. Introduction

II. Experimental and Theoretical Methods

A. Introduction

B. Computational Approaches to Adsorption/Reaction

- Embedded Cluster Models
- Quantum Cluster Models

III. Development of Theory and Novel applications

New embedded Cluster Models

- Chemical Physics Letters, 350 (2001) 128-134.

IV. Environmental Catalysis

Adsorption of CO, NO_x, on Metallosilicate Zeolites

- Journal of Physical Chemistry B 2001,105, 2421-2428.
- Surface Science and Catalysis, 2001, 135, 2518-2525.
- Journal of Molecular Catalysis, 2000, 153,155.
- Journal of Molecular Structure, 2000, 525, 155.

V. Adsorption/Reaction in Zeolites:

Reactions and mechanisms of molecular probes on Faujasite:

- Surface Science and Catalysis, 2001, 135, 2469-2476.
- Journal of Molecular Structure, 2001, 560, 167-177.

VI. Physical Organic Chemistry of solid catalysts:

Hydrocarbon Transformation:

- Chemical Physics Letters, 2001, 349, 161-166.

VII. Summary and Conclusions

VIII. Acknowledgements

I. Introduction

Rational catalyst design, notably nanostructural materials, represents one of the most rewarding challenges in chemical research. Zeolites have been used as catalysts in many industrial processes, in addition to many other uses due to their nanostructured framework. They play a significant role in chemicals and fuels production. Their physicochemical properties are based on the ability of the open framework structures to enclose metals [Fe, Cu Ag, Pt, etc.], charged and neutral species as well as nanocluster with in cavities. These nonstructural catalysts can be tailored or tuned to maximize the product of target molecules by employing state-of-the-art techniques.

The Brønsted acidity of zeolitic catalysts generated from surface hydroxyl within their framework is of prime importance and has led to numerous important industrial applications, such as catalysts and adsorbents which have been employed for petrochemical processes and for the production of fine chemicals. Of particular interest in this active research is the adsorption structure of methanol and water and the question of whether these probe molecules are protonated or not at acid zeolite catalysts are discussed in depth. In spite of a large volume of documents about zeolite research, the details of structures and reaction mechanisms of adsorption, and particularly of protonation/deprotonation are still incomplete and, mainly, to be solved.

Transition metal zeolite catatalyst, Cu-ZSM-5, has been the subject of many recent theoretical and experimental studies since it was discovered to thermally and photoactivated catalyze the reduction of NOx species.[1-7] The adsorption of NO molecules on the active site to form nitrosyl complexes is considered the important step. Much progress in understanding the nature of the active site of the Cu-ZSM-5 zeolite has been made. However, a detailed molecular-level understanding of the mechanism of catalytic reduction of NOx species is far from complete. XANES, EXAFS, and photoluminescence showed that Cu(I) species are the active site for the decomposition of NO,8-12 and almost all of Cu(II) ions in Cu-ZSM-5 can be autoreduced to Cu(I) ions during an evacuation process.9 CO has been frequently used as a probe molecule to obtain information about the active sites of Cu-ZSM-5 due to its high IR absorbance intensity and the stability of the Cu-ZSM-5/CO complexes.10,13-15 CO is known to be adsorbed on Cu-ZSM-5, even under mild conditions such as at low pressure and room temperature.[16-23] The frequency shift of CO in the adsorption complex has been used to depict the characteristic of the active site and its bonding nature. At least two types of Cu(I) species had been identified from previous IR experiments.[16,17,24] The first Cu(I) species bonds symmetrically to two framework oxygen atoms, and the other bonds asymmetrically to three framework oxygen atoms. Those results agree with

XAFS, IR, and UV-vis spectroscopy studies, which showed that the average coordination number of Cu(I) is 2.5 (0.3.8-11,25 Experimental observations suggested that the first Cu(I) type is an active site for the NOx adsorption, but both types are required for the NOx decomposition process.

Numerous theoretical models have also been performed to provide information on the nature of the active site of Cu- ZSM-5. Several models of the active site have been proposed from the simplest model, in which a Cu cation is in fixed coordination with water ligands (Cu+[H2O]n),[26-28] to more realistic ones which consist of up to six tetrahedral sites.[18,29-35] As discussed below, these models have some mix success. Furthermore, although its coordination information has been established, the location of Cu+ in the zeolite framework is not known for certain. Previous HF and lattice energy minimizing calculations showed that T12 is the most stable site for Al substitution and is believed to be the type I active center.[36,37] Such a site is reasonable from the structural point of view, since the bridging oxygens adjacent to the T12 site protrude into the intersection of main and sinusoidal channels; thus, this site provides sufficient space for small adsorbates binding to the exchanged copper ion.38 For this reason, most previous theoretical works have chosen T12 as the active site's center. However, using a more accurate combined quantum/potential methodology, Sauer and co workers showed that T12 is not the most stable site for Al,[39] though it is among the more stable sites and there are only negligible differences in the relative energies of these sites. This issue certainly requires further study.

Understanding the adsorption of CO and NO on Cu-ZSM-5 zeolite would be the first step in studying the catalytic activity of this zeolite. Experimentally, the 2156-2157 cm-1 band was attributed to the stretching frequency of adsorbed CO on the Cu(I) site.[9,15,17,24,40] Kuroda deconvoluted this peak into two dominant peaks at 2159 and 2151 cm-1, which were assigned to the stretching frequencies of CO adsorbed at Cu(I) species binding to two and three oxygen atoms, respectively. When Cu- ZSM-5 is exposed to NO gas, there are three bands appearing via IR at 2295, 1630, and 1812 cm-1. The first two bands occur due to spontaneous decomposition of NO, and the last band was attributed to NO adsorbing on the Cu+ site.[8,9,16,41,42] The experimental binding energies of CO and NO largely depend on many factors, e.g., the Si/Al ratio, the Cu exchanged rate, temperature, and pressure. The relative binding energy between CO and NO is still questionable. However, recent IR and adsorption experiments suggested that CO molecules bind to Cu-ZSM-5 zeolite stronger than NO molecules.[24,43] Adsorption of CO and NO have also been the subject of numerous theoretical studies.[18,27-30,34,35,44-50] The calculated results for adsorption energy, frequency shift, geometry, and the coordination number are still scattered due to differences in the topological structure of the model, cluster size, constraints, basis sets, and the levels of theory employed. Almost all of the previous theoretical models, except the Cu-water cluster, were not able to predict the experimental blue shift of adsorbed CO. Although the simplest Cu+[H2O]n model was able to illustrate several important characteristics of the active site, including the frequency shift of adsorbed CO, the predicted NO and CO binding energies are far below the experimental heat of adsorption values.[51]

One of the most important characteristics of zeolite is its complicated framework comprising of channels and pores. The simplest approximation is to only consider the active site locally and ignore the environment effects of the zeolite framework, as in the cluster model. However, there is sufficient evidence that such environment effects are significant.[5,15,52,53] For instance, the framework of ZSM-5 significantly enhances the catalytic property of Cu-ZSM-5 over other Cu-exchanged zeolites. So we cannot refute the important role of the

Zeolite framework in this catalytic process. From a computational point of view, to account for the effects of the zeolite framework in the study of adsorption or reactions in zeolites has been a great challenge. The large unit cells of most zeolites, such as 288 atoms for the ZSM-5, prevent the use of an accurate periodic electronic-structure method, though some progress has been made in this direction, but at a great computational cost.[54-61] It should be noted that periodic calculations correspond to high loading (coverage) cases.

A practical approach to account for the crystal effects of the zeolite is to embed the quantum mechanical cluster model of the active site in a classical potential field due to the extended zeolite framework. There are two embedding approaches. One is referred to as the electronic embedding method, which includes the electrostatic interactions of the infinite lattice of zeolite in the Fock matrix of a quantum mechanic cluster.[62-66] The other is referred to as the mechanical embedding method, which represents with an analytical force field the potential from the crystal environment and the active site is treated as a quantum mechanical cluster.[45,39,67,68] Although there are some differences in these two approaches, both have been successfully applied to studying adsorptions and reactions in zeolites. It is interesting to note that to date there has not been a systematic theoretical study focusing on the dependence of NO and CO adsorption properties on models of the active site, i.e., cluster size, Madelung potential, levels of theory.

From a theoretical point of view, to gain a qualitative understanding on the adsorption of small molecules on metalexchanged zeolite, one first needs to have some knowledge on the model dependence of adsorption properties of interest. In this study, our main objectives are (1) to provide a better understanding of the cluster and embedded cluster computational methodology in the study of adsorption/reaction in metalexchanged zeolites and (2) to predict adsorption properties for adsorption of NO and CO on Cu-ZSM-5 zeolite. The focus of our first objective is on the cluster size dependence and the effects of the Madelung potential on the NO/CO adsorption properties. This is accomplished by carrying out both cluster and embedded cluster calculations for different quantum clusters representing the active center. The focus of our second objective is on the adsorption structures, energies, and frequency shifts of the NO/CO adsorbed complexes. The results of this study are important for establishing a cost-effective methodology for future studies on the mechanisms of both thermal and photoactivated catalytic reductions of NOx by Cu-ZSM-5 and other metal-exchanged -ZSM-5 zeolites.

II. Experimental and Theoretical Methods

Modeling reactivity of catalysts has been a theoretical challenge. Our focus has been to design structure, sorption and reaction dynamics in catalytic systems using Electronic Structure Cluster and Electronic Embedded Cluster methods. In this new electronic embedded cluster methodology, the active site is modeled as a reactive cluster embedded in a long-range electrostatic effect of the zeolitic crystal. This allows the active site to be carried out at an accurate level of electronic structure theory while the influence of zeolite crystal is effectively included. Combining this with the conventional cluster method will provide us a powerful tool to predict reaction mechanisms in catalysts.

Several interesting problems, namely adsorption, proton siting, and reactions of hydrocarbon in nanostructural catalysts been investigated.

III. Development of Embedded Cluster Models and Their Novel Applications to Catalysis

Embedded methodologies have been suggested to close the gap between the cluster approach and the periodic calculation. They are considered not only because the cluster models need corrections for neglected interactions with their surroundings but also because they are a promising alternative to the use of supercells in periodic calculations. In this approach interactions between the adsorbate species may give undesired effects, unless the supercells become prohibitively large. A cluster containing the active site is defined and the corresponding wave function is calculated in such a way that a smooth link is attained with the wave function of the surrounding crystal.

When dealing with the adsorption of molecules on metal surfaces in a cluster approach, serious problems arise. The requisite of electron localization at atoms or in bonds, which allows for treatment of ionic or covalent materials in a well-defined way, is no longer valid for metals. We note, however, that the method required to perform an ab initio calculation of the whole embedding part and computational benefits are only achieved when calculations of higher quality (better basis set, inclusion of electron correlation) are made for the embedded part.

A hybrid method that treats the region the adsorption takes place quantum-mechanically and embeds it in the infinite host crystal, which is described by a classical model

Attempts have been made and are being made to improve the cluster model by including corrections for the external long-range potential, Vext(r), into the calculation. This leads to terms such as

$$F_{\mu\nu} = F^{\circ}_{\mu\nu} + \left\langle \mu(r) \middle| V_{ext}(r) \middle| \nu(r) \right\rangle$$

in the Fock matrix elements $F_{\mu\nu}$ The fixed external potential Vext may be defined according to Hermann as represented by a superposition of contributions V_i (r) centered at substrate atom sites R^i,

$$V_{ext}(\mathrm{r}) = \sum_i V_i(r - R_i)$$

Each V_i is given by a multipolar expansion, envisaging multipole moments q_{LM} and spherical harmonics $Y_{LM}(r)$,

$$V_i(r) = \sum_{LM} (q_{iLM} / r^{L+1}) Y_{LM}(r)$$

It is, however, very common to restrict the multipoles to point charges or, at most, to charges plus dipoles. From a computational point of view, the increase in computer time due to inclusion of the external potential in an SCF procedure is very modest, because only extra one-electron integrals are needed and virtually all quantum mechanical packages allow for the addition of an array of charges in a straightforward way.

The different embedding schemes differ by the way the multipoles q_{iLM} are determined and the one-electron integrals $\langle \mu(r) | V_{ext}(r) | \nu(r) \rangle$ are evaluated.

(1) A CRYSTAL calculation of the substrate is performed and the nonexpanded electrostatic potential, $V^{crystal}(r)$, is derived from the periodic wave function in the region where adsorption takes place. A cluster model is chosen, adopting the same structure, and the molecular electrostatic potential, $V^{cluster}(r)$, is evaluated from the cluster wave function in the same region. (1a) The difference of the values of these two potentials is then least-square-fitted to the classical electrostatic potential of a finite number of point charges, located, e.g., at substrate ion positions (point ion cluster, PIC) outside the quantum mechanical cluster

$$V^{ext}(r) = V^{crystal}(r) - V^{cluster}(r) = \sum_i^{PIC} q_i / (r - R)$$

The best fit is obtained by varying the values of the charges, keeping their location fixed. An example is the scheme of Greatbanks et al. (1b) The charge density of the crystal and the cluster are partitioned according to a generalized Mulliken scheme which allows for expression of the electrostatic potentials of the crystal and the cluster, respectively, in terms of atomic multipole contributions. The external potential is obtained as the difference of the two potentials:

$$V^{ext}(r) =$$

$$\sum_i^{crystal} \sum_{LM} (q_{iLM}{}^{crystal} / r^{L+1}) Y_{LM}(r - R_i) -$$

$$\sum_i^{cluster} \sum_{LM} (q_{iLM}{}^{cluster} / r^{L+1}) Y_{LM}(r - R_i)$$

i.e., no fitting is involved. However, to avoid numerical errors, the summation does not include the atoms of a well-defined inner zone of the cluster and the crystal (in which the adsorption takes places). It is assumed that the charge distributions of the cluster and the periodic crystal do not differ in this zone. Similarly, the correction term $\langle \mu(r) | V_{ext}(r) | \nu(r) \rangle$ is only added to the Fock matrix if both atomic orbitals, μ and ν, are centered on nuclei belonging to the inner zone. This scheme suggested by Teunissen et al. offers a solution to two important problems: (i) It reduces the artificial polarization of the charge

distribution by the external potential in the outer zone of the cluster where Pauli repulsion is not preventing such effects. (ii) It eliminates contributions to the calculated binding energy of the adsorbed species, which are due to the terminating atoms introduced to saturate dangling bonds but are not present in the real crystal.

(2) Simpler schemes start from the Madelung potential for the bulk crystal using charges estimated from population analysis of cluster calculations or from chemical considerations. For example, full ion charges may be chosen for partially ionic solids such as SiO2. The value of the embedding charges may even be treated as free parameters in order to assess the sensitivity of the results to different Madelung potentials.

There are two ways to include point charges into a Fock operator:

(2a) as an Ewald sum, consisting of a direct space term (from which the charges of the cluster atoms should be subtracted) plus a reciprocal space term, and

(2b) as a finite number of point charges. The charge value and/or the positions of some of these charges may be adjusted to reproduce the exact Madelung potential. The former approach needs special one-electron integrals while the latter requires trival modifications of existing codes only. Scheme 2b has also been used to embed clusters with saturation atoms, but the choice of the Point charges was not trival. The saturating atoms themselves contribute to the potential felt by the interior atoms of the cluster and, to avoid exceedingly large polarization, embedding point ions should not be placed very close to the bordering atoms.

A new electronic embedded technique: SCREEP

Surface Charge Representation of External Embedding Potential

To accurately calculate the Madelung potential of a crytal, one requires an infinite Ewald summation over point charges in the 3-D crystal. Implementing such a summation within the Hartree-Fock formalism is not simple. Furthermore, derivative of the Ewald sum is difficult to evaluate. The SCREEP method is designed to replace to the Ewald sum by a sum over a small finite number of point charges. To do this, we first imagine a piece of conductor in an arbitrary external potential field. Electrons in the conductor will rearrange on the surface of this conductor so that the TOTAL potential on the surface or anywhere inside the conductor is vanished, namely

$$V_{ext}(r) + \oint_S \frac{\sigma(r')d^2r'}{|r'-r|} = 0 \qquad (1)$$

Where r and r' are on the surface S, σ (r) is the surface charge distribution. The above boundary condition gives us a way to replace the external potential

calculated from the Ewald sum by a surface charge distribution. It is important to note that the quantum cluster or physical system does not have to be a conductor. We use the conductor boundary as a mathematical trick to replace the Madelung potential by a surface charge distribution. In practice we discritize the surface charge distribution into a finite set of point charges. To minimize the error in doing so, we divide the Madelung potential into two parts. The potential from the point charges that are close to the quantum cluster will have a large fluctuation in the magnitude and sign and thus will be treated explicitly. This leaves the remaining external potential smoother on the surface S, and thus discritization would have smaller error. Equation (1) becomes

$$\mathbf{V}'_{ext} + \mathbf{qA} = 0 \qquad (2)$$

where $\mathbf{V}'_{ext}$ is the remaining Madelung potential at the locations of the surface charges, $\mathbf{q}$ is the finite number of surface charges, and A is the inverse distance matrix. Solving this matrix equation will give you q. The surface charge representation of the external embedding potential is

$$\mathbf{q}^{screep} = -\mathbf{q}$$

Specification to Adsorption/Reaction of H2O cluster over Faujasitic Catalyst

Cluster and embedded cluster models were used to determine the structure of water molecules adsorption of zeolites $[H_3SiOHAl(OH)_2OSiH_3]/[H_2O]_n$; n = 1-4 and their possible ion-pair species. The cluster is selected to model specially to faujasite zeolite with the symmetry C1. In models employed, the dangling bonds of "surface" oxygen atoms are terminated by H atom and Si-H bonds are aligned with the corresponding Si-O bonds of the structure of faujasite Zeolite.

In the embedded cluster model, the static Madelung potential due to atoms outside of the quantum cluster was represented by partial atomic charges located at the zeolite lattice sites. Charges close to the quantum cluster are treated explicitly while the Madelung potential from the remaining charges from an infinite lattice is represented by a set of surface charges that were derived from the Surface Charge Representation of External Electrostatic Potential (SCREEP) method. In this study, the total Madelung potential is represented by 1137 explicit charges and 146 surface charges. With this small number of point charges, additional computational cost is often less than 5% compared to bare cluster calculations.

Specification to Environmental Catalysis: Adsorption of CO, NOx, on Metallosilicate Zeolites

The ZSM-5 structure was taken from the silicious ZSM-5 crystal (Figure 1a).69 To represent the Lewis basic active site, the silicon atom of the T12 site was substituted by an aluminum atom. Note that we selected the T12 site for this study for the reason discussed above. An Cu(I) ion was added to counterbalance the negative charge of [AlO4]-. The exchanged monovalent copper ion was chosen to bind to two framework oxygen atoms (corresponding to the I2 site in ref 39), protruding in to the channel intersection as an initial guess structure.

Four clusters ranging from 3T to 10T, where T is Si- or Al tetrahedral (SiO_4 or AlO_4^-), were cut from the ZSM-5 lattice. The largest cluster, [AlSi9O16H20]-Cu+, is a complete 10 membered-ring cluster of the main channel of ZSM-5 (Figure 1b). This model represents the zeolite's pore structure, enclosing an active site and adsorbates. The other clusters are 7T, 5T, and 3T that have molecular structures of [AlSi6O12H16]-Cu+, [AlSi4O10H12]-Cu+, and [AlSi2O8H8]-Cu+, respectively (see Figures 1c-e). Due to the partial covalent nature of zeolite, the boundary Si atoms of each cluster were saturated by capped hydrogen atoms located along the broken Si-O bonds in ZSM-5 lattice with a Si-H bond distance of 1.47 Å. The boundary SiH_3 groups were held fixed in all geometry optimizations.

To incorporate the environmental effects of the remaining zeolite framework, the QM clusters are embedded in a potential field of point charges. The SCREEP method was used to construct these point charges. The detailed description of the SCREEP method was previously discussed elsewhere.64 To account for the electrostatic potential from the capped hydrogen atoms and to minimize their interactions with the external point charges, we removed the first shell of external charges closest to the QM cluster and adjusted the charge's values of the next shell to reproduce the correct classical Madelung potential calculated from the Ewald-sum method in the active site region.

Nonlocal hybrid density functional theory, particularly the B3LYP functional, was used in this study due to its consistency and reliability in zeolite systems.[31,34,45,66,70] For practical purpose, we employed a larger basis set for the active site region, [SiOAlOSi]-Cu+, namely, the 6-31G(d) basis set for Si, Al, O, and the adsorbate; the HayWadt-VDZn+1 ECP basis set for Cu(I) ion; and the smaller 3-21G basis set for the remaining spectator region.

Preliminary calculations for the smaller embedded model confirmed the experimental observation that adsorptions of CO and NO do not have large effects on the structure of the Zeolite framework.[51,66] Thus, to reduce the computational demand the active site and the surrounding sites, except those of the SiH_3 boundary groups, were allowed to fully relax in both cluster and embedded cluster calculations and then were held fixed in subsequent NO/CO adsorption calculations. All calculations were done using the Gaussian98 program.[71]

Specification to Physical Organic Chemistry of solid catalysts: Hydrocarbon Transformation:

We used a 3T cluster, namely SiH3OHAl(OH)2OSiH3, for the bare cluster calculations. For the embedded cluster model, this 3T cluster is embedded in a set of point charges according to the Surface Charge Representation of External Embedded Potential (SCREEP) method. Accuracy of this method for modeling adsorption processes in zeolites has already been addressed in our previous studies. The SCREEP embedded cluster model used in this study consists of three layers. The center layer is tri-tetrahedral (3T) quantum chemical cluster. The next layer of the model is a set of explicit point charges that were derived from periodic population analysis on zeolite systems. To minimize the errors due to the interactions that occur between the quantum mechanical terminating hydrogens and the neighboring point charges, the layer of explicit point charge nearest to the quantum cluster is moved out and combined with the next layer of point charges. The charge values of the moved point charges are fitted to minimize deviation from the original external electrostatic field. The outermost layer of the model is the SCREEP surface, which is represented by a set of a small number of surface point charges to represent the remaining Madelung potential from the extended zeolite crystal. In the H-FAU, the total Madelung potential is represented by 1137 explicit charges within 3.5 Å to the quantum cluster and 146 surface charges, whereas for the H-ZSM-5, 201 explicit charges and 688 surface charges are employed for representing the potential. Note that pure SiO2 FAU and ZSM-5 crystal structures were used in calculating the Madelung potential thus Si/Al ration effects are not included in this study.

All calculations were done at the B3LYP level using 6-31G (d, p) basis using the Gaussian98 program [17]. In all geometry optimizations the capped H atoms of the two SiH3 groups and the two OH groups bonded to the Al atom are fixed along the Si-O crystal framework of the zeolite [18] while other atoms in the quantum cluster are allowed to relax. For the adsorption complex, both the adsorbate and the active site are optimized. This effectively accounts for the local structure relaxation due to the Al substitution in creating the Brønsted acid site and to interaction with the adsorbate. It is known that DFT does not account for the dispersion component of the interactions, single point MP2/6-31G (d,p) calculations were carried out at the B3LYP optimized geometries to improve the energetic information between ethylene and the zeolite framework.

III.

Development of Theory and Novel applications

New Embedded Cluster Models

- **Chemical Physics Letters, 350 (2001) 128-134.**

14 December 2001

ELSEVIER

Chemical Physics Letters 350 (2001) 128–134

CHEMICAL PHYSICS LETTERS

www.elsevier.com/locate/cplett

A full quantum embedded cluster study of proton siting in chabazite

Piti Treesukol [a,b], James P. Lewis [a], Jumras Limtrakul [b], Thanh N. Truong [a,*]

[a] *Department of Chemistry, Henry Eyring Center for Theoretical Chemistry, University of Utah, 315 S 1400 E, rm 2020, Salt Lake City, UT 84112, USA*

[b] *Laboratory for Computational and Applied Chemistry, Chemistry Department, Kasetsart University, Bangkok 10900, Thailand*

Received 10 July 2001; in final form 9 October 2001

Abstract

We propose a computational strategy within the full quantum embedded cluster methodology for modeling reactivity in extended systems. This method takes advantages of the embedded cluster methodology for treating interactions in the active region accurately while allowing interactions with the remaining crystal framework to be treated fully quantum mechanically by using the ab initio tight-binding theory. We have applied this method to study proton siting in chabazite. We found that our calculated relative stability of proton at four different oxygen sites agree well with those from previously periodic calculations, though the computational demand for the present approach is much less. © 2001 Elsevier Science B.V. All rights reserved.

1. Introduction

Despite rapid advances in computer technology and tremendous efforts in improving the efficiency of electronic structure methods, modeling reactivity in extended systems remains a challenge for quantum chemistry [1,2]. Periodic electronic structure methods provide an accurate framework to model interactions in extended systems such as crystals or surfaces. For porous materials such as zeolites, the unit cells are often larger than 100 heavy atoms. In such a case, the use of accurate periodic electronic structure methods is rather limited. A number of periodic density functional theory (DFT) studies of interactions in zeolites have been reported recently but only for small zeolitic systems [3–11]. These periodic DFT calculations used enormous computational resources.

Alternatively there are two other computational methodologies that are often employed, namely the cluster and embedded cluster methods. The cluster methodology treats the active region surrounding the active site (or defects) and the adsorbate quantum mechanically as an isolated system and totally ignores the effects of the remaining crystal framework. In many cases, such a treatment is sufficient in providing useful insights. However, there is sufficient evidence that the effects of the remaining crystal lattice, mainly the

* Corresponding author. Fax: +1-801-581-4353.
E-mail address: truong@chem.utah.edu (T.N. Truong).

0009-2614/01/$ - see front matter
PII: S0009-2614(01)01277-5

Madelung potential, are crucial for obtaining quantitative understanding on the mechanism of chemical processes that occur at the active sites (or defects) of the crystal. The embedded cluster methodology [12–17] takes advantages of the simplicity of the cluster approach but adds the effects of the crystal framework in an approximated manner. Two approximations known as the electronic embedding [12,14–17] and mechanical embedding [13] approaches have been developed. Both approaches have shown to perform quite well for many studies on adsorption and reactions at the Brønsted active sites of zeolites. Both, however, have inherent fundamental approximations. The electronic embedding neglects the crystal polarization and long-range structure relaxation effects whereas the mechanical embedding neglects the direct polarization of the wavefunction representing the active region and assumes certain accuracy of the potential force field, which was fitted to QM cluster results.

In this study we present a new computational strategy within the full quantum embedded cluster (FQEC) methodology that takes advantages of the embedded cluster methodology for accurate treatment of the active region and of the periodic electronic structure methods for rigorous representation of interactions in the extended system. Several different computational strategies within this general full quantum embedded methodology have been previously proposed [11,18,19]. The proposed computational strategy has its unique strength in crystals with large unit cells such as zeolites. For this reason, we select proton siting in H-chabazite as a model system for assessing its accuracy.

2. Methodology

The central idea of the embedded cluster methodology is to divide the physical system into two regions, the active and spectator regions. Most existent embedded cluster methods are based on the QM/MM methodology. In the present approach, the spectator region is also treated quantum mechanically by a periodic electronic structure theory. The partition of the physical system within the periodic boundary condition is illustrated in Fig. 1. The total energy of the system can be expressed within the framework of the ONIOM methodology developed by Morokuma and co-workers [20]

$$E_{\text{tot}} = E^{\text{Low}}_{\text{crystal}} + \left(E^{\text{High}}_{\text{cluster}} - E^{\text{Low}}_{\text{cluster}}\right) + \Delta E_{\text{boundary}}. \quad (1)$$

A physical interpretation for Eq. (1) is followed. In the first term, interactions in all regions, the active and spectator regions of the crystal and the cross-term interactions between the two regions are represented within a low level of periodic quantum mechanical formalism. The second term represents the correction to the local interactions

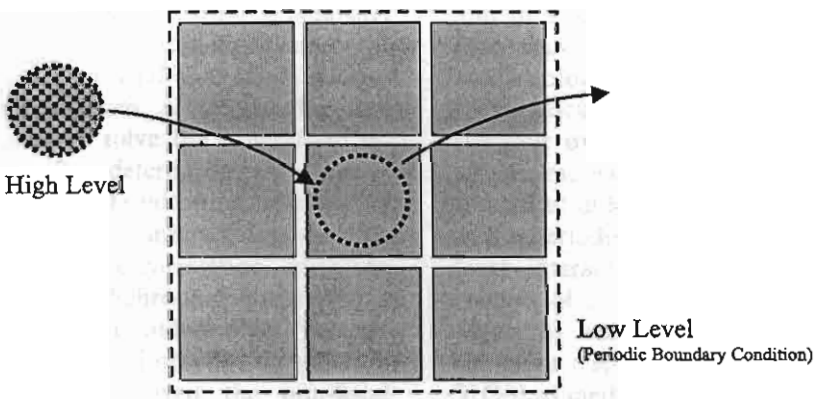

Fig. 1. Schematic description of the full quantum embedded cluster methodology.

in the active region by a more accurate level of electronic structure theory. The last term represents the difference in the energy of the boundary region calculated at the two levels of theory. With careful choice of the boundary region, the last term can be made to remain nearly constant in a chemical process and thus has no effect on the relative energy; consequently it can be ignored. We have shown that the ONIOM approach as in Eq. (1) can be used to improve the prediction for the adsorption energy of H_2O on $Al_2O_3(0001)$ surface calculated from our electronic embedded cluster method [21]. Sauer and co-workers also used the same energy correction expression both within the QM/MM methodology as in the QM–pot method [13] and within the full quantum embedded cluster methodology in their more recent study [11].

Correction for the local interactions in the active region can be done at any level of quantum chemistry methods available for isolated systems. Since we can correct the interactions in the most important region, it is possible to use a less accurate periodic electronic structure method to model interactions in the crystal. For the crystal energy term and the third term in Eq. (1), we propose to use the ab initio self-consistent tight-binding (AITB) method developed by Sankey and co-workers [22,23] called FIREBALL. The advantage of using this method is that systems with unit cells of order 1000 atoms can be easily considered on a Pentium III-based workstation. This is in fact the key strength of the present approach.

This AITB method is based on the generalized norm-conserving separable pseudopotentials of the Hamann type within a self-consistent density functional theory formalism. A tight-binding-like Hamiltonian is used to solve the generalized eigenvalue equation for determining the band-structure energy. This Hamiltonian consists of different density-functional interactions (i.e. kinetic, Coulomb, exchange-correlation, etc.). In solving the one-electron Schrödinger equation a set of slightly excited pseudoatomic 'fireball' wavefunctions are used. For the application discussed below, we employed the non-local Becke exchange and Lee-Yang-Parr correlation functional (BLYP) and the double numerical (DN) basis set of the sp^3 type. For convenience in the discussion below, we introduce a notation for AITB calculations similar to quantum chemistry methods for isolated systems, namely AITB calculations with the BLYP functional using the DN basis set as AITB(BLYP)/DN. The development of the DN basis set and the technical aspects of the AITB method have been described previously [23]. For the FQEC calculations, we used the ONIOM notation, i.e., high level:low level.

3. Test system and computational details

To test the proposed method we have applied it to study proton siting in H-chabazite. Due to its small unit cell of 37 atoms, several theoretical studies [3,5,8–11] using different periodic electronic structure methods have been carried out for the proton siting in this zeolite. Results from these studies are valuable for comparison purposes here. For chabazite, all tetrahedral sites (T-sites) (Al or Si tetrahedral sites) are equivalent by symmetry. At a given Al T-site, the Brønsted proton can reside on any of the four non-equivalent neighboring oxygen (O_1 through O_4) atoms as shown in Fig. 2a. Since these oxygen atoms are non-equivalent in the zeolite framework, Brønsted protons at different sites have different physical properties such as acidity and stability. In other words, the effect of the zeolite framework is perhaps the sole factor that distinguishes the differences among these sites and thus the relative stability of proton at these four sites provides a stringent test of the new methodology.

To calculate the relative stability of proton at the four oxygen sites, four different H-chabazite structures, where the Brønsted acidic proton is located at different sites, were first fully optimized at the periodic AITB(BLYP) level. To correct the local interactions near the Brønsted acid site, clusters of 13T surrounding the four oxygen sites (Fig. 2b) were selected from the optimized H-chabazite structures. The hybrid B3LYP/6-31G(d,p) method was used as the high level in this test case.

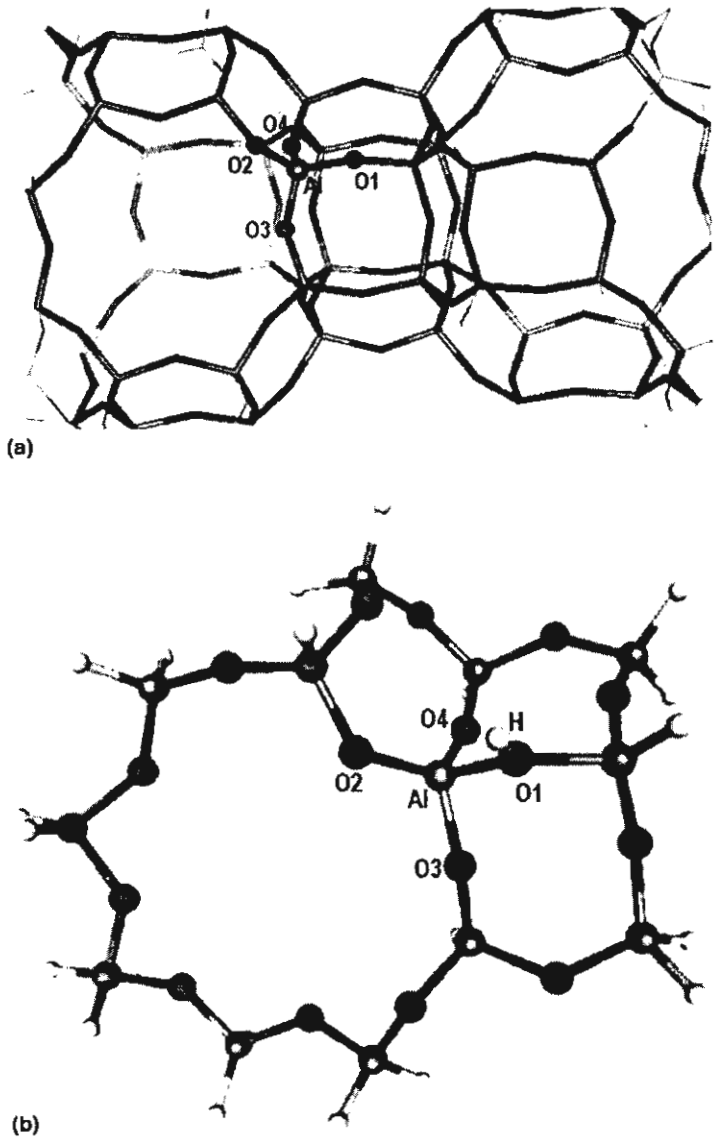

Fig. 2. (a) Perspective view of four non-equivalent oxygen atoms in the chabazite framework. (b) 13T cluster used in FQEC calculations.

4. Results and discussion

4.1. Structure relaxation

Brønsted acidic site is created when the Si atom at a tetrahedral site is substituted by an Al atom. Due to the change in the valency at the tetrahedral site, one can expect such a substitution would induce a large structure relaxation on the zeolite framework. As expected we found a large structure relaxation upon Al substitution in chabazite from the periodic AITB calculations. Selected optimized geometrical parameters are listed in Table 1 along with those from previous studies. The degree of relaxation is different when the proton is located at one of the four different neighbor oxygen sites. In particular, the Si–O bond distance in the chabazite SiO_2 crystal lattice is 1.65 Å. Upon substitution,

Table 1
Selected structural parameters of Brønsted acid sites in H-chabazites (Å and degree)

H-site	Method	O–H	Si–O(H)	Al–O(H)	∠Al–O(H)–Si	OUT(OH)[a]
O1	Periodic AITB	1.007	1.748	1.894	121.0	9.7
	QM-pot[b]	0.976	1.725	1.910	128.4	2.8
	Periodic DFT[c]	0.974	1.702	1.904	132.9	0.6
	Periodic DFT[d]	0.972	1.680	1.838	132.8	–
O2	Periodic AITB	1.004	1.723	1.846	129.7	8.0
	QM-pot[b]	0.977	1.721	1.876	133.4	12.3
	Periodic DFT[c]	0.976	1.701	1.876	135.2	20.5
	Periodic DFT[d]	0.971	1.681	1.807	132.6	–
O3	Periodic AITB	1.011	1.714	1.858	139.9	3.8
	QM-pot[b]	0.978	1.722	1.883	134.0	5.3
	Periodic DFT[c]	0.976	1.697	1.876	136.8	13.7
	Periodic DFT[d]	0.973	1.678	1.808	134.1	–
O4	Periodic AITB	1.059	1.748	1.912	148.9	1.9
	QM-pot[b]	0.980	1.738	1.921	129.9	7.4
	Periodic DFT[c]	0.975	1.714	1.938	135.2	11.6
	Periodic DFT[d]	0.972	1.697	1.857	134.4	–

[a] Out-of-plane angle.
[b] Taken from [3].
[c] Taken from [8].
[d] Taken from [9].

the Al–O(H) bond distance (O(H) is the oxygen atom of the hydroxyl group) varies from 1.846 to 1.912 Å. The large elongation in this particular lattice bond creates a local strain to the framework and induces changes in coordinates of the nearby atoms, particularly the Al–O(H)–Si angle. This angle is compressed from the original value of about 145° by as much as 26°.

The Al–O(H)–Si angle can be used to compare the differences between different computational methods in predicting the crystal structure relaxation upon Al substitution. It is interesting to note that the QM–pot method was able to reproduce the large structure relaxation upon Al substitution [3]. The variation in the magnitude of such relaxation when the Brønsted acidic proton located at four different sites is rather small as indicated by the range in the Al–O(H)–Si angle from 128° to 134° as compared to the range 121–149° from the periodic AITB calculations. However, the plane-wave periodic DFT results have a much smaller range 133–137° [8]. In our periodic AITB calculations, experimental crystal parameters from SiO_2 chabazite crystal (volume of 798 $Å^3$) were used. Periodic plane-wave DFT calculations [8] have shown that upon Al substitution the unit-cell volume is expanded from 800 to 821 $Å^3$. Thus, constraining the unit-cell volume at 798 $Å^3$ would introduce an external pressure on the system and thus would induce larger structure changes. That is in fact observed in our AITB calculations. Optimizing the crystal parameters using the periodic AITB method is being carried out and the results will be reported in a forthcoming paper.

Table 2
Relative stability for the Brønsted acidic proton located at the four distinct oxygen atoms O1–O4 in the active site of chabazite

Methods	Relative energy (kcal/mol)			
	O1	O2	O3	O4
Periodic AITB(BLYP)	0.00	3.78	3.99	3.81
Cluster AITB(BLYP)[a]	10.49	8.08	0.00	0.33
Cluster B3LYP[a]	8.50	6.65	0.00	5.28
B3LYP:AITB//AITB	0.00	4.35	5.98	10.75
Periodic HF//QM–pot[b]	0.00	4.07	3.09	3.01
Periodic HF[c]	(0.0)	(16.0)	(76.7)	(80.1)
Periodic DFT//QM–pot[d]	(0.0)	2.75	1.72	3.21
Periodic DFT[e]	0.00	2.10	1.25	1.43
Periodic DFT[f]	0.00	1.61	0.92	2.08
CCSD(T):DFT//QM–pot[g]	0.00	9.00	5.20	12.90

[a] Using 13T clusters selected from the periodic AITB(BLYP)/DN optimized crystal structures.
[b] Taken from [5].
[c] Taken from [10]; partial optimization; site specific information was not given explicitly.
[d] Taken from [3].
[e] Taken from [8].
[f] Taken from [9].
[g] Taken from [11].

4.2. Energetics

Relative stability for the Brønsted acidic proton located at the four distinct oxygen atoms O1–O4 (denoted as H1–H4, respectively) in the active site of chabazite calculated by different methods is listed in Table 2. Our calculated results can be compared to those from previous periodic HF// QM–pot [5], B3LYP//QM–pot [3,11] and plane-wave PZPW91 [8,9] calculations. Larin and Vercauteren [10] reported a periodic HF study with partial optimization for this system. All periodic methods including the present periodic AITB and B3LYP:AITB ones predict H1 to be the most stable. This is in consistent with the observation from a powder neutron diffraction study that found two distinct acid sites at O1 and O3 in the unit cell [24]. Different methods, however, yield slightly different order of relative stability for the remaining sites H2–H4. The differences in the spread of relative stability between B3LYP:AITB results of 10.7 kcal/mol and those of periodic HF// QM–pot, B3LYP//QM–pot, and plane-wave PZPW91 results of less than 4.1 kcal/mol can be due to (1) the degree of structure relaxation upon Al substitution in chabazite discussed above and/ or (2) the differences in the local interactions. The later is supported by the recent the periodic DFT study when the interaction in the active region (1T) is corrected at the CCSD(T) level the larger spread of 12.9 kcal/mol was observed [11].

Results from AITB and B3LYP single-point energy calculations for 13T clusters used in the determination of the B3LYP:AITB energy can also provide information on the contributions of the electronic component of the zeolite framework, local interactions, and structure relaxation in the relative stability of proton at these four sites. First of all, comparing the cluster and periodic AITB results, we found that the electronic component of the zeolite framework, i.e. Madelung potential and crystal polarization, has a significant effect on the relative stability of the H1–H4 Brønsted acidic protons. Without it, the AITB method predicts the H3 and H4 protons to be more stable while H1 and H2 protons to be much higher in energy. This is in fact totally opposite to results from periodic calculations. In particular, this component stabilizes the H1–H4 protons by 14.5, 8.3, 0.0, and 0.5 kcal/mol relative to that of the H3 proton, respectively. Comparing the B3LYP and AITB cluster results, we found that improving the accuracy for interactions in the active site region stabilizes the H1 and H2 protons by 2.0 and

1.4 kcal/mol, respectively, while it destabilizes the H4 proton by 5.0 kcal/mol relative to that of the H3 proton. Thus the local corrections for interactions in the active region further spread the relative stability of these protons as mentioned above.

5. Conclusion

We presented a computational strategy within the full quantum embedded cluster (FQEC) methodology for studying reactivity of extended systems. This method takes advantages of the embedded cluster methodology for treating interactions in the active region accurately while allowing interactions with the remaining crystal framework to be treated fully quantum mechanically but at a less accurate level, particularly by the use of an ab initio tight-binding theory. To illustrate the applicability and accuracy of this method, we performed a study on proton siting in chabazite. The non-local hybrid B3LYP level of theory was used for the active region while a self-consistent tight-binding AITB method was used for determining the crystal structure when the Brønsted proton is located at four different oxygen atoms O1–O4 in the active site. We found that the FQEC results are consistent with previously published full periodic HF and DFT results. This is particularly encouraging since the present approach is computationally much less demanding compared to the periodic HF or DFT methods, thus allowing consideration of crystals with large unit cells such as zeolites. Furthermore, the availability of analytical gradient and Hessian for the AITB method opens many opportunities for the FQEC method in studying reactivity of extended systems. This study so far only provides proof of the concept. More studies however are required to fully access its range of applicability and limitations. Such studies are currently being considered in our lab.

Acknowledgements

This work is supported in part by the Thailand Research Fund, ACS Petroleum Research Fund, the National Science Foundation, and the Science and Technology Higher Education Development Project funded by the MUA-ADB. The computer support from the Center of High Performance Computing at University of Utah is gratefully acknowledged.

References

[1] R.A. van Santen, G.J. Kramer, Chem. Rev. 95 (1995) 637.
[2] C.R.A. Catlow (Ed.), Modeling of Structure and Reactivity in Zeolites, Academic Press, San Diego, 1992.
[3] M. Sierka, J. Sauer, J. Chem. Phys. 112 (2000) 6983.
[4] J.-R. Hill, C.M. Freeman, B. Delley, J. Phys. Chem. A 103 (1999) 3772.
[5] M. Brändle, J. Sauer, J. Chem. Phys. 109 (1998) 10379.
[6] E.H. Teunissen, C. Roetti, C. Pisani, A.J.M. deMan, A.P.J. Jansen, R. Orlando, R.A. vanSanten, R. Dovesi, Model. Sim. Mater. Sci. Eng. 2 (1994) 921.
[7] L. Campana, A. Selloni, J. Weber, A. Pasquarello, I. Papai, A. Goursot, Chem. Phys. Lett. 226 (1994) 245.
[8] Y. Jeanvoine, J.G. Angyan, G. Kresse, J. Hafner, J. Phys. Chem. B 102 (1998) 5573.
[9] R. Shah, J.D. Gale, M.C. Payne, Phase Transitions 61 (1997) 67.
[10] A.V. Larin, D.P. Vercauteren, J. Mol. Catal. A 168 (2001) 123.
[11] M. Sierka, J. Sauer, J. Phys. Chem. B 105 (2001) 1603.
[12] M. Allavena, K. Seiti, E. Kassab, G. Ferenczy, J.G. Angyan, Chem. Phys. Lett. 168 (1990) 461.
[13] M. Brändle, J. Sauer, J. Mol. Catal. A 119 (1997) 19.
[14] T. Bredow, G. Geudtner, K. Jug, J. Chem. Phys. 105 (1996) 6395.
[15] S.P. Greatbanks, P. Sherwood, I.H. Hillier, J. Phys. Chem. 98 (1994) 8134.
[16] C. Pisani, U. Birkenheuer, Int. J. Quantum Chem. S 29 (1995) 221.
[17] E.V. Stefanovich, T.N. Truong, J. Phys. Chem. B 102 (1998) 3018.
[18] N. Govind, Y.A. Wang, A.J.R. da Silva, E.A. Carter, Chem. Phys. Lett. 295 (1998) 129.
[19] E.V. Stefanovich, T.N. Truong, J. Chem. Phys. 104 (1996) 2946.
[20] M. Svensson, S. Humbel, K. Morokuma, J. Chem. Phys. 105 (1996) 3654.
[21] V. Shapovalov, T.N. Truong, J. Phys. Chem. B 104 (2000) 9859.
[22] O.F. Sankey, D.J. Niklewski, Phys. Rev. B 40 (1989) 3979.
[23] J.P. Lewis, K.R. Glaesemann, G.A. Voth, J. Fritsch, A.A. Demkov, J. Ortega, O.F. Sankey, Phys. Rev. B 64 (2001) 195103.
[24] L.J. Smith, A. Davidson, A.K. Cheetham, Catal. Lett. 49 (1997) 143.

IV.

Environmental Catalysis

Adsorption of CO, NO_x, on Metallosilicate Zeolites

- Journal of Physical Chemistry B 2001,105, 2421-2428.
- Stud. Surf. Sci. Catal, 2001, 135, 2518-2525.
- Journal of Molecular Catalysis, 2000, 153,155.
- Journal of Molecular Structure, 2000, 525, 155.

Adsorption of Nitrogen Monoxide and Carbon Monoxide on Copper-Exchanged ZSM-5: A Cluster and Embedded Cluster Study

Piti Treesukol,[1,2] Jumras Limtrakul,[2] and Thanh N. Truong[1]

[1]*Henry Eyring Center for Theoretical Chemistry, Department of Chemistry, University of Utah, 315 S. 1400 E., rm. 2020, Salt Lake City, Utah 84112, and* [2]*Department of Chemistry, Faculty of Science, Kasetsart University, Jatujak, Bangkok 10900, Thailand*

Received: November 22, 2000; In Final Form: January 17, 2001

We present a systematic study on the adsorption of NO and CO in Cu−ZSM-5, using an ab initio embedded cluster methodology at the B3LYP level of theory. We found that the effects of the cluster size and Madelung potential are small for adsorption energies of CO and NO. For adsorption of CO, the calculated binding energy of 32 kcal/mol is in good agreement with experimental data from 29 to 32 kcal/mol. On the contrary, for adsorption of NO the calculated binding energy of 22 kcal/mol is much smaller than the experimental estimate, though it is consistent with recent experimental observation that NO binding energy should be smaller than that of CO. Madelung potential, however, is important for obtaining the correct blue shift of an adsorbed CO and red shift of an adsorbed NO.

Introduction

Cu−ZSM-5 has been the subject of many recent theoretical and experimental studies since it was discovered to thermally and photoactivated catalyze the reduction of NO_x species.[1−7] The adsorption of NO molecules on the active site to form nitrosyl complexes is considered the important step. Much progress in understanding the nature of the active site of the Cu−ZSM-5 zeolite has been made. However, a detailed molecular-level understanding of the mechanism of catalytic reduction of NO_x species is far from complete.

XANES, EXAFS, and photoluminescence showed that Cu(I) species are the active site for the decomposition of NO,[8−12] and almost all of Cu(II) ions in Cu−ZSM-5 can be autoreduced to Cu(I) ions during an evacuation process.[9] CO has been frequently used as a probe molecule to obtain information about the active sites of Cu−ZSM-5 due to its high IR absorbance intensity and the stability of the Cu−ZSM-5/CO complexes.[10,13−15] CO is known to be adsorbed on Cu−ZSM-5, even under mild conditions such as at low pressure and room temperature.[16−23] The frequency shift of CO in the adsorption complex has been used to depict the characteristic of the active site and its bonding nature. At least two types of Cu(I) species had been identified from previous IR experiments.[16,17,24] The first Cu(I) species bonds symmetrically to two framework oxygen atoms, and the other bonds asymmetrically to three framework oxygen atoms. Those results agree with XAFS, IR, and UV−vis spectroscopy studies, which showed that the average coordination number of Cu(I) is 2.5 ± 0.3.[8−11,25] Experimental observations suggested that the first Cu(I) type is an active site for the NO_x adsorption, but both types are required for the NO_x decomposition process.

Numerous theoretical models have also been performed to provide information on the nature of the active site of Cu−ZSM-5. Several models of the active site have been proposed from the simplest model, in which a Cu cation is in fixed-coordination with water ligands $(Cu^+[H_2O]_n)$,[26−28] to more realistic ones which consist of up to six tetrahedral sites.[18,29−35] As discussed below, these models have some mix success. Furthermore, although its coordination information has been established, the location of Cu^+ in the zeolite framework is not known for certain. Previous HF and lattice energy minimizing calculations showed that T12 is the most stable site for Al substitution and is believed to be the type I active center.[36,37] Such a site is reasonable from the structural point of view, since the bridging oxygens adjacent to the T12 site protrude into the intersection of main and sinusoidal channels; thus, this site provides sufficient space for small adsorbates binding to the exchanged copper ion.[38] For this reason, most previous theoretical works have chosen T12 as the active site's center. However, using a more accurate combined quantum/potential methodology, Sauer and co workers showed that T12 is not the most stable site for Al,[39] though it is among the more stable sites and there are only negligible differences in the relative energies of these sites. This issue certainly requires further study.

Understanding the adsorption of CO and NO on Cu−ZSM-5 zeolite would be the first step in studying the catalytic activity of this zeolite. Experimentally, the 2156−2157 cm^{-1} band was attributed to the stretching frequency of adsorbed CO on the Cu(I) site.[9,15,17,24,40] Kuroda deconvoluted this peak into two dominant peaks at 2159 and 2151 cm^{-1}, which were assigned to the stretching frequencies of CO adsorbed at Cu(I) species binding to two and three oxygen atoms, respectively. When Cu−ZSM-5 is exposed to NO gas, there are three bands appearing via IR at 2295, 1630, and 1812 cm^{-1}. The first two bands occur due to spontaneous decomposition of NO, and the last band was attributed to NO adsorbing on the Cu^+ site.[8,9,16,41,42] The experimental binding energies of CO and NO largely depend on many factors, e.g., the Si/Al ratio, the Cu exchanged rate, temperature, and pressure. The relative binding energy between CO and NO is still questionable. However, recent IR and adsorption experiments suggested that CO molecules bind to Cu−ZSM-5 zeolite stronger than NO molecules.[24,43] Adsorption of CO and NO have also been the subject of numerous

10.1021/jp004280g CCC: $20.00
Published on Web 03/03/2001

theoretical studies.[18,27-30,34,35,44-50] The calculated results for adsorption energy, frequency shift, geometry, and the coordination number are still scattered due to differences in the topological structure of the model, cluster size, constraints, basis sets, and the levels of theory employed. Almost all of the previous theoretical models, except the Cu−water cluster, were not able to predict the experimental blue shift of adsorbed CO. Although the simplest $Cu^+[H_2O]_n$ model was able to illustrate several important characteristics of the active site, including the frequency shift of adsorbed CO, the predicted NO and CO binding energies are far below the experimental heat of adsorption values.[51]

One of the most important characteristics of zeolite is its complicated framework comprising of channels and pores. The simplest approximation is to only consider the active site locally and ignore the environment effects of the zeolite framework, as in the cluster model. However, there is sufficient evidence that such environment effects are significant.[5,15,52,53] For instance, the framework of ZSM-5 significantly enhances the catalytic property of Cu−ZSM-5 over other Cu-exchanged zeolites. So we cannot refute the important role of the zeolite framework in this catalytic process. From a computational point of view, to account for the effects of the zeolite framework in the study of adsorption or reactions in zeolites has been a great challenge. The large unit cells of most zeolites, such as 288 atoms for the ZSM-5, prevent the use of an accurate periodic electronic-structure method, though some progress has been made in this direction, but at a great computational cost.[54-61] It should be noted that periodic calculations correspond to high loading (coverage) cases.

A practical approach to account for the crystal effects of the zeolite is to embed the quantum mechanical cluster model of the active site in a classical potential field due to the extended zeolite framework. There are two embedding approaches. One is referred to as the electronic embedding method, which includes the electrostatic interactions of the infinite lattice of zeolite in the Fock matrix of a quantum mechanic cluster.[62-66] The other is referred to as the mechanical embedding method, which represents with an analytical force field the potential from the crystal environment and the active site is treated as a quantum mechanical cluster.[45,39,67,68] Although there are some differences in these two approaches, both have been successfully applied to studying adsorptions and reactions in zeolites. It is interesting to note that to date there has not been a systematic theoretical study focusing on the dependence of NO and CO adsorption properties on models of the active site, i.e., cluster size, Madelung potential, levels of theory.

From a theoretical point of view, to gain a qualitative understanding on the adsorption of small molecules on metal-exchanged zeolite, one first needs to have some knowledge on the model dependence of adsorption properties of interest. In this study, our main objectives are (1) to provide a better understanding of the cluster and embedded cluster computational methodology in the study of adsorption/reaction in metal-exchanged zeolites and (2) to predict adsorption properties for adsorption of NO and CO on Cu−ZSM-5 zeolite. The focus of our first objective is on the cluster size dependence and the effects of the Madelung potential on the NO/CO adsorption properties. This is accomplished by carrying out both cluster and embedded cluster calculations for different quantum clusters representing the active center. The focus of our second objective is on the adsorption structures, energies, and frequency shifts of the NO/CO adsorbed complexes. The results of this study are important for establishing a cost-effective methodology for future studies on the mechanisms of both thermal and photo-activated catalytic reductions of NO_x by Cu−ZSM-5 and other metal-exchanged -ZSM-5 zeolites.

Methodology

The ZSM-5 structure was taken from the siliceous ZSM-5 crystal (Figure 1a).[69] To represent the Lewis basic active site, the silicon atom of the T12 site was substituted by an aluminum atom. Note that we selected the T12 site for this study for the reason discussed above. An Cu(I) ion was added to counterbalance the negative charge of $[AlO_4]^-$. The exchanged monovalent copper ion was chosen to bind to two framework oxygen atoms (corresponding to the I2 site in ref 39), protruding in to the channel intersection as an initial guess structure.

Four clusters ranging from 3T to 10T, where T is Si- or Al-tetrahedral (SiO_4 or AlO_4^-), were cut from the ZSM-5 lattice. The largest cluster, $[AlSi_9O_{16}H_{20}]^-Cu^+$, is a complete 10-membered-ring cluster of the main channel of ZSM-5 (Figure 1b). This model represents the zeolite's pore structure, enclosing an active site and adsorbates. The other clusters are 7T, 5T, and 3T that have molecular structures of $[AlSi_6O_{12}H_{16}]^-Cu^+$, $[AlSi_4O_{10}H_{12}]^-Cu^+$, and $[AlSi_2O_8H_8]^-Cu^+$, respectively (see Figures 1c−e). Due to the partial covalent nature of zeolite, the boundary Si atoms of each cluster were saturated by capped hydrogen atoms located along the broken Si−O bonds in ZSM-5 lattice with an Si−H bond distance of 1.47 Å. The boundary SiH_3 groups were held fixed in all geometry optimizations.

To incorporate the environmental effects of the remaining zeolite framework, the QM clusters are embedded in a potential field of point charges. The SCREEP method was used to construct these point charges. The detailed description of the SCREEP method was previously discussed elsewhere.[64] To account for the electrostatic potential from the capped hydrogen atoms and to minimize their interactions with the external point charges, we removed the first shell of external charges closest to the QM cluster and adjusted the charge's values of the next shell to reproduce the correct classical Madelung potential calculated from the Ewald-sum method in the active site region.

Nonlocal hybrid density functional theory, particularly the B3LYP functional, was used in this study due to its consistency and reliability in zeolite systems.[31,34,45,66,70] For practical purpose, we employed a larger basis set for the active site region, $[SiOAlOSi]^-Cu^+$, namely, the 6-31G(d) basis set for Si, Al, O, and the adsorbate; the HayWadt-VDZ_{n+1} ECP basis set for Cu(I) ion; and the smaller 3-21G basis set for the remaining spectator region.

Preliminary calculations for the smaller embedded model confirmed the experimental observation that adsorptions of CO and NO do not have large effects on the structure of the zeolite framework.[51,66] Thus, to reduce the computational demand the active site and the surrounding sites, except those of the SiH_3 boundary groups, were allowed to fully relax in both cluster and embedded cluster calculations and then were held fixed in subsequent NO/CO adsorption calculations. All calculations were done using the Gaussian98 program.[71]

Results and Discussion

In this study, we have examined both the physical properties of CO and NO adsorptions on Cu−ZSM-5 zeolite and the factors that can affects the accuracy of the embedded cluster model, particularly the size of the quantum cluster and the Madelung potential. Thus it is natural to separate the discussion of the results into two parts, namely, model dependence and chemistry of CO and NO adsorption on Cu−ZSM-5 zeolite.

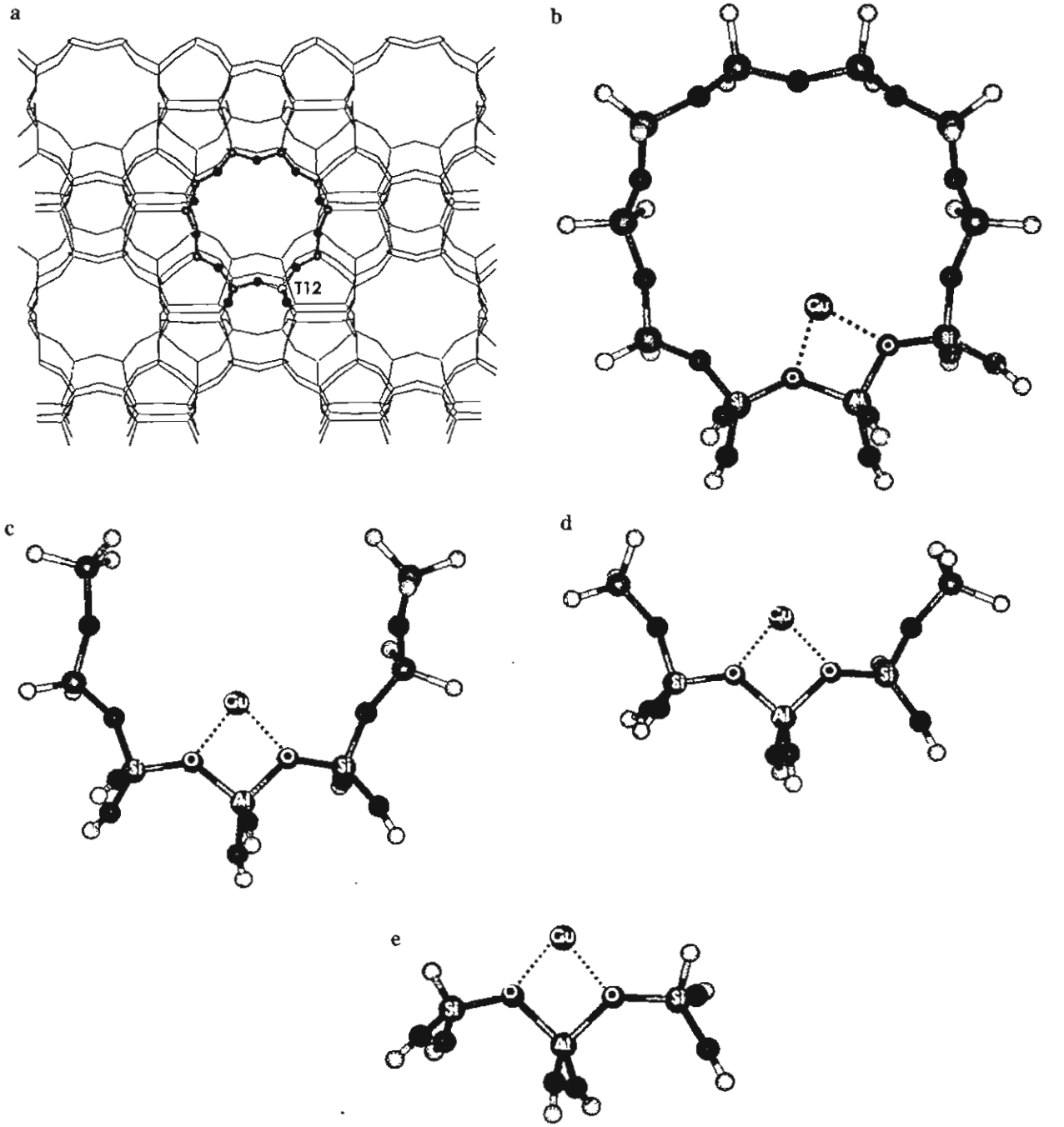

Figure 1. Cu−ZSM-5 Cluster models: (a) ZSM-5 lattice, (b) 10T cluster, (c) 7T cluster, (d) 5T cluster, and (e) 3T cluster of Cu−ZSM-5.

Our calculated results are summarized in Tables 1−3. Optimized geometrical parameters, Mulliken charges, and Cu ion binding energy of Cu−ZSM-5 calculated from both the cluster and embedded cluster methods using four different QM clusters are tabulated in Table 1. Similar results for CO and NO adsorption on Cu−ZSM-5 are listed in Tables 2 and 3, respectively.

Model Dependence. In the embedded cluster methodology, there are two main factors that can affect the accuracy of the results, namely, the size of the QM cluster and the representation of the embedded potential. It is difficult to separate the effects of these two factors. In this study, the embedding potential consists of only the long-range electrostatic contribution from the zeolite framework. As the size of the QM cluster increases, it includes the short-range electrostatic, repulsion-dispersion, and polarization contributions from the local region of the active site in its full quantum mechanical treatment. Thus, the most accurate results from this study are from the embedded 10T cluster calculations and are used as a reference point for comparison in the discussion of model dependence.

Cu−ZSM-5 Active Site. We found that the local structure of the active site, i.e., the Cu^+ ion binding site, is not very sensitive to the size of the QM cluster and the inclusion of the Madelung potential. As the size of the QM cluster increases from 3T to 10T, the Cu−O bond distances increase by at most 0.01 Å and the Al−O (to O1 or O2) bond distances decrease by at most 0.05 Å. The Cu−Al distance appears to converge at

TABLE 1: Structural Parameters (Å), Mulliken Charges (au), and Binding Energy (kcal/mol) of Cu-ZSM-5 Clusters

	3T			5T			7T			10T		
MFI	bare	emb[a]	emb[b]	bare	emb[a]	emb[b]	bare	emb[a]	emb[b]	bare	emb[a]	emb[b]
Cu−O1[c]	1.980		2.003	1.990		2.006	1.994		2.012	1.998		2.013
Cu−O2[c]	1.993		2.005	2.010		2.016	2.011		2.023	2.012		2.032
Cu−Al	2.743		2.767	2.725		2.748	2.732		2.758	2.732		2.764
Al−O1	1.812		1.819	1.752		1.760	1.752		1.755	1.751		1.753
Al−O2	1.780		1.785	1.748		1.757	1.747		1.748	1.748		1.745
q(Cu)	0.52	0.61	0.61	0.52	0.57	0.58	0.49	0.55	0.55	0.48	0.55	0.55
q(O)	−0.60	−0.60	−0.59	−0.60	−0.60	−0.60	−0.60	−0.60	−0.59	−0.60	−0.60	−0.60
E_{bind}(Cu)[d]	180.13		233.76	184.02		195.62	185.76		180.05	187.30		163.90

[a] Unoptimized embedded cluster. [b] Optimized embedded cluster. [c] Framework oxygens. [d] Includes BSSE correction.

TABLE 2: Structural Parameters (Å and deg), Mulliken Charges (au), and Binding Energy (kcal/mol) of CO Adsorption on Cu-ZSM-5 Clusters

	Cu(I)	3T		5T		7T		10T	
	C-down	O-down	C-down	C-down		C-down		C-down	
parameters[a]	cluster	emb	cluster	emb	cluster	emb	cluster	emb	cluster	emb
CO[b]	1.126	1.139	1.137	1.136	1.138	1.134	1.138	1.135	1.137	1.136
Cu−C(O)	1.893	2.002[e]	1.818	1.827	1.815	1.829	1.817	1.829	1.825	1.832
∠Cu−CO	179.9	175.9[f]	179.8	178.8	180.0	178.6	178.2	174.7	178.6	177.8
q(CO)	0.26	0.13	0.22	0.25	0.23	0.25	0.23	0.25	0.23	0.24
q(Cu)	0.74	0.54	0.36	0.43	0.33	0.37	0.30	0.36	0.29	0.37
q(O$_z$)[c]		−0.60	−0.60	−0.60	−0.60	−0.60	−0.60	−0.60	−0.60	−0.60
E_{bind}[d]	57.50	6.18	32.58	32.21	32.53	32.83	32.98	33.13	31.69	32.30

[a] Only the adsorbate is optimized. [b] Optimized gas-phase CO bond length is 1.138 Å. [c] Average of charges on two bridging oxygen atoms. [d] Include BSSE and ZPE corrections. [e] Cu−O(C) distance. [f] ∠Cu−OC.

TABLE 3: Structural Parameters (Å and deg), Mulliken Charges (au), and Binding Energy (kcal/mol) of NO Adsorption on Cu-ZSM-5 Clusters

	Cu(I)	3T		5T		7T		10T	
	N-down	O-down	N-down	N-down		N-down		N-down	
parameters[a]	cluster	emb	cluster	emb	cluster	emb	cluster	emb	cluster	emb
NO[b]	1.147	1.174	1.168	1.166	1.169	1.164	1.168	1.165	1.167	1.165
Cu−N(O)	1.871	1.952[e]	1.815	1.822	1.814	1.826	1.815	1.823	1.821	1.824
∠Cu−NO	179.9	138.1[f]	145.4	145.4	144.8	144.8	145.3	147.6	148.0	148.3
q(NO)	0.12	0.10	0.08	0.11	0.09	0.13	0.09	0.13	0.10	0.12
q(Cu)	0.88	0.54	0.45	0.52	0.43	0.45	0.40	0.44	0.38	0.46
q(O$_z$)[c]		−0.59	−0.59	−0.59	−0.59	−0.59	−0.59	−0.59	−0.59	−0.59
E_{bind}[d]	42.94	7.32	23.38	22.84	23.66	22.80	23.92	23.47	22.61	21.78

[a] Only the adsorbate is optimized. [b] Optimized gas-phase NO bond length is 1.159 Å. [c] Average of charges on two bridging oxygen atoms. [d] Include BSSE and ZPE corrections. [e] Cu−O(N) distance. [f] ∠Cu−ON.

7T. Examining the convergence of the structural parameters, we found that the 3T cluster results deviate noticeable from others, thus indicating such a cluster is too small. Inclusion of the Madelung potential increases all Cu−O, Al−O, and Cu−Al bond distances. The largest variation of about 0.03 Å is in the Cu−Al bond distance. The increase in the Cu−Al bond distance would hinder the delocalization of Cu^+ charge by the zeolite framework. This observation is further supported by the larger Cu Mulliken charge (by 0.1 au) when the Madelung potential is included (see Figure 2). Note that increasing the cluster size in bare cluster calculations does not have such an effect. Thus, the Cu^+ charge localization is due mainly to the Madelung potential. The Cu^+ binding energy shows the largest dependence on both the QM cluster size and the Madelung potential. From the bare cluster calculations, the Cu^+ binding energy increases from 180.1 to 187.3 kcal/mol when the size of the QM cluster increases from 3T to 10T. The embedded calculations show the reverse trend, i.e., the binding energy decreases from 233.8 to 163.9 kcal/mol from the 3T to the 10T case. This indicates that inclusion of only the long-range Madelung potential may overestimate the Cu^+ binding energy. The local short-range repulsion dispersion and polarization of the zeolite framework also have a noticeable contribution in lowering the ion binding energy.

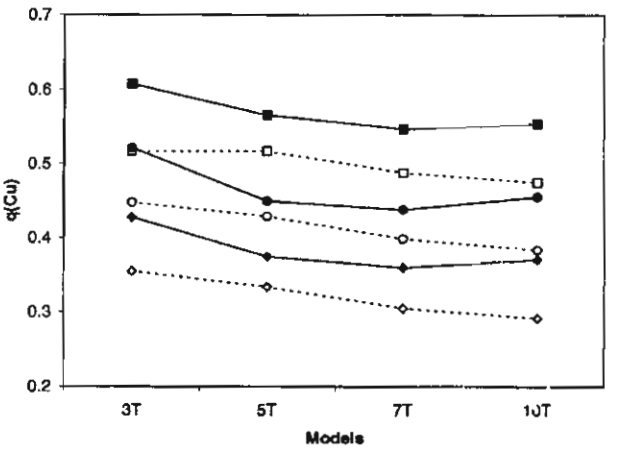

Figure 2. The cluster size and the Madelung potential dependences of the Cu Mulliken charge: cluster (□), embedded cluster (■), CO/cluster (○), CO/embedded cluster (●), NO/cluster (◇), and NO/embedded cluster (◆).

CO and NO Adsorption. Both CO and NO may bind to a Cu ion of Cu−ZSM-5 via either the C- (or N-) down or the O-down structures. The results are shown in Tables 2 and 3. We have used both bare and embedded 3T cluster models to investigate both modes of adsorption for CO and NO on Cu−ZSM-5. For both systems, the Cu−O binding distances (Cu to oxygen of CO or NO) in the O-down adsorption complexes are more than 0.13 Å longer than the corresponding C-down or N-down case. Consequently, the O-down adsorption complexes have much weaker binding energies, particularly 6.2 versus 33.2 kcal/mol for the CO/Cu−ZSM-5 complex and 7.3 versus 22.8 kcal/mol for the NO/Cu−ZSM-5 complex. For this reason, we do not expect that the O-down adsorption mode would play an important role in the chemistry of reduction of NO_x by Cu−ZSM-5 zeolite, and thus, we only concentrate our further efforts to study the C-down and N-down adsorption modes.

It is interesting to note that the structures and binding energies for adsorption of both CO and NO on Cu−ZSM-5 zeolite do not depend strongly on either the cluster size or the Madelung potential. In fact, variations in the CO and NO bond distances in the adsorption complexes are less than 0.005 Å for both bare and embedded cluster methods. Inclusion of the Madelung potential is seen to lengthen the adsorption distance (Cu−N or Cu−C bond distance) by at most 0.015 Å. Similar to the Cu−ZSM-5 zeolite, in the adsorption complexes, the Madelung potential localizes the Cu^+ ion charge but to a lesser degree. Both the effects of the QM cluster size and the Madelung potential give rise to the variations in the CO binding energy from 31.7 to 33.2 kcal/mol and in the NO binding energy from 21.8 to 23.9 kcal/mol. It is interesting to point out the general perception that the Madelung potential tends to increase the binding energy of the adsorbate. It is not so. Our results show that the Madelung potential increases the CO binding energy by about 1 kcal/mol but decreases the NO binding energy also by about 1 kcal/mol. Although the effect of the Madelung potential is not large here, it is sufficient to illustrate the point.

In summary, with the exception of the Cu^+ ion binding energy, the structures of the Cu−ZSM-5 and its CO and NO adsorption complexes and their corresponding binding energies exhibit a rather weak dependence on the size of the quantum cluster and the inclusion of the Madelung potential. The Madelung potential, however, was found to stabilize the Cu^+ ion charge and thus reduces the charge delocalization by the zeolite framework. This would have an important implication in studying the photocatalytic activity of metal-exchanged zeolites where the charge-transfer process is thought to be an important step in the catalytic cycle. From the variations in the structures, binding energies, and Mulliken charges, we found that the embedded 5T cluster model provides a balance between computational efficiency and accuracy.

Chemistry. In this subsection, we discuss the chemistry of CO and NO adsorption on Cu−ZSM-5 and comparisons of our results with those from previous experimental and other theoretical studies. For this, we use the results from our most accurate embedded 10T cluster calculation.

Cu−ZSM-5. Previous experimental and theoretical studies have suggested that Cu^+ ions are located at intersections between sinusoidal and main channels, exposed to diffused species. The majority of Cu^+ ions in ZSM-5 are expected to coordinate to two bridging oxygen atoms of the active site.[18,29,30,33,45,50,72] All structural parameters of our model, i.e., bond distances and the coordination number of the copper ion, are comparable to experimental results. Particularly, the calculated Cu−O bond distances of 2.013−2.032 Å (see Table 1) are in excellent agreement with the experimental data of 2.00 ± 0.02 Å, determined by Lamberti et al.[8] In comparison with previous theoretical studies, our calculated Cu−O bond distances are slightly larger. In particular, Chakraborty et al.,[33] using the 5T cluster, found the two Cu−O bond lengths of 1.95 and 1.86 Å. The DFT/LSD calculations of Hass and Schneider on the 5T cluster yielded Cu−O distances of 1.919 and 1.924 Å.[30] Increasing cluster size and including the Madelung potential do not have large effects, though they bring the results in better agreement with experimental values. Although there is some charge redistribution between the copper ion and zeolite framework, the charge of 0.55 on the Cu^+ ion supports the suggestion that these Cu^+ ions prefer to exist as isolated monomer species.[73]

Since experimental data for the Cu^+ binding energy is not available, we compare our results to previous theoretical data. We mentioned above that the binding energy between the Cu^+ cation and zeolite framework shows a strong dependence on the cluster size and the Madelung potential. Comparisons with previous studies further support this conclusion and also show some dependence on the levels of theory employed. In particular, Hass and Schneider used the simple 5T model at the DFT/LSDA level of theory and obtained the binding energy of 175 kcal/mol.[29] Sauer and co-workers[45] determined the Cu^+ binding energy of 160 kcal/mol from a 3T model at the DFT/B3LYP level of theory. Sauer et al.[39] also predicted a value of 148.6 kcal/mol from their mechanical embedded 3T cluster model (QM-pot) at the same level of theory. Our calculated binding energy with the basis set superposition error (BSSE) correction is 164 kcal/mol. The variations in these results serve as a caution for the use of cluster and embedded cluster models in studying Lewis basic sites and adsorption of ions on zeolites.

Adsorption of CO on Cu−ZSM-5. Basically, the nature of the bonding between a Cu^+ ion and a CO molecule can be described by the back-bonding process. The HOMO orbital of CO is the $5\sigma^*$ antibonding orbital. σ donation from this orbital to the transition metal ion would strengthen both the CO bond and the Cu−CO interaction. On the other hand, the LUMO of CO is the $6\pi^*$ orbital. π accepting to this orbital, i.e., electron flows from the transition metal to the $5\pi^*$ orbital, would strengthen the Cu−CO interaction but weaken the CO bond.

CO bond length is shortened slightly upon adsorption. Our calculated $Cu-O_{framework}$ and Cu−C distances of 2.03 and 1.832 Å are in excellent agreement with those of 2.05 and 1.89 Å determined by Nagao et al.[51] using spectroscopic techniques. As expected, the Cu−C bond is slightly affected by the Madelung potential, thus supporting the observation that the Cu−C stretching frequency is much more sensitive to the zeolite structure, i.e., the long-range potential, than the CO bonding.[15] The Cu−CO angle is linear (Figure 3) corresponding to previous calculation studies.[26,27,30] The net charge of the adsorbed CO molecule is slightly positive, revealing the electron transfer from an adsorbate to the copper ion. From the shortening of the CO bond length and the decreasing of the Cu^+ positive charge, we can conclude that the σ donating dominates the interaction between the exchanged copper and the carbonyl ligand.

One of the most important characteristics of the CO/Cu−ZSM-5 complex that can be obtained from experiment is the IR frequency of adsorbed CO. While the interaction between the bare Cu^+ ion and a CO molecule yields the red shift of the CO stretching frequency, IR spectra of adsorption of CO on Cu−ZSM-5 yields two peaks (from two different Cu^+ sites as mentioned above) at 2159 and 2151 cm^{-1}, which are blue-shifted from the peak at 2143 cm^{-1} of the gas-phase CO.[24] This

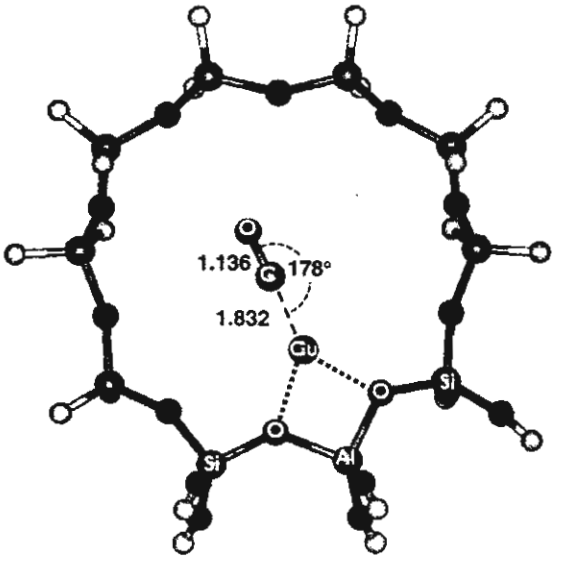

Figure 3. Optimized structure of CO/Cu−ZSM-5 complex using the embedded 10T model.

blue shift should correspond to the stronger and shorter CO bond, as observed in this study. To confirm this the stretching frequency of an adsorbed CO was calculated using our embedded 3T model. Without any scaling, the adsorbed CO frequency was determined to be 2237.7 cm^{-1}, blue-shifted from 2208.2 cm^{-1} of the gas-phase CO. Such a blue shift was not observed in most of the previous theoretical models, even at the same cluster size and the same level of calculation. Thus the Madelung potential is expected to be important for obtaining the correct blue shift of an adsorbed CO.

The binding energies calculated from previous theoretical models are quite scattered, ranging from 25 to 54 kcal/mol.[27,29,30,46,74] The experimental CO binding energy was determined to be 28.7 kcal/mol by Nagao et al.[51] and 31.6 kcal/mol by Szanyi and Paffett (an unpublished result cited by Brand et al.[27]). After including the BSSE correction and zero-point energy (ZPE) correction, we obtain the CO binding energy of 32.01 kcal/mol, which agrees well with experimental values.

In this study, we found an "anticorrelation" between binding energy and bond distance. If the bonding between an ion and an adsorbate is dominated by electrostatic interaction, one can expect that the binding energy decreases upon increasing the bond distance. Our results show that while the binding energy between the bare Cu^+ ion with CO (57.5 kcal/mol) is much larger than that (32.3 kcal/mol) of the Cu−ZSM-5/CO complex, the Cu−C bond distance is longer, 1.893 Å compared to 1.832 Å. This indicates that the interactions between the Cu^+ site in ZSM-5 zeolite and CO are more complex than just an electrostatic one. This supports the previous suggestion that the combination of electrostatic interaction, between CO molecule and zeolitic framework, and σ donation, between CO and exchanged copper ion, induces a blue shift of adsorbed CO.[75]

Adsorption of NO on Cu−ZSM-5.

The HOMO of NO molecule is the $6\pi^*$ orbital. The electron transfer from the copper's d-orbital to this orbital in the π accepting process increases the Cu^+−NO interaction but simultaneously decreases the NO bond order, i.e., elongates the NO bond distance while the π and σ donating (from $5\sigma^*$ and $6\pi^*$ orbitals) would increase the Cu^+−NO interaction and NO bond order, i.e., shorten the NO bond distance.

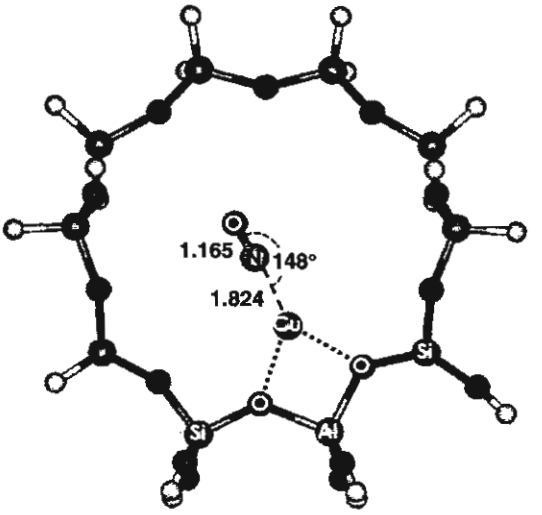

Figure 4. Optimized structure of NO/Cu−ZSM-5 complex using the embedded 10T model.

Our calculated NO bond distance in the NO/Cu−ZSM-5 complex is 1.165 Å, which is longer than the gas-phase value of 1.159 Å. Previous theoretical studies have also observed this elongation of the NO bond. This indicates that π accepting is the dominant process, which is opposite of the CO/Cu−ZSM-5 case. It is interesting to point out that for the bare Cu^+ ion/NO complex, the NO bond distance is shortened to 1.147 Å and thus σ donating is preferred (molecular charge of adsorbed NO compared to free NO). These results show that the zeolite framework is important in determining the nature of the bonding between the exchanged Cu^+ ion and the adsorbate. From IR studies, the NO stretching vibration at 1810 cm^{-1} was assigned to linearly adsorbed NO, since generally NO frequencies that are larger than 1720 cm^{-1} correspond to linear species.[18,76,77] Our Cu−NO angle of 148° (see Figure 4) differs drastically from this suggestion and also from the CO/Cu−ZSM-5 case (see Figure 3). This appears to be a contradiction between our result and experiment. Since the interaction between the Cu^+ ion and NO is dominated by the π accepting, one can expect that the Cu−NO configuration should be bent to have a positive overlap with Cu's d orbital (the linear configuration would yield zero-overlap). This is different from the CO/Cu−ZSM-5 system, where the σ donating is the dominant process and the linear configuration would have the largest overlap. To further understand the difference between our result and the experimental observation, we plotted a potential curve as the function of the Cu−NO angle, as shown in Figure 5. From the overlap argument above one can expect the linear configuration to be the saddle point between the two symmetrical bent structures. Figure 5 confirms our expectation, and the barrier for converting between the two stable bent structures is only 1 kcal/mol.[26] This suggests that experiments would observe the average of the thermal fluctuation between the two stable bent structures, i.e., the linear configuration. Thus, our results provide a deeper understanding of the adsorption structure of NO on Cu−ZSM-5.

The NO stretching frequency of the NO/Cu−ZSM-5 complex, observed experimentally at 1812 cm^{-1}, is red-shifted from 1860 cm^{-1} of the gas-phase NO.[42] This red shift corresponds to the lengthening of the NO bond, observed in our study and other theoretical works.[27,29,32,46,47] The stretching frequency of an adsorbed NO was calculated using our embedded 3T model to be 1921.7 cm^{-1}, red-shifted from 1990.4 cm^{-1} of the gas-phase NO.

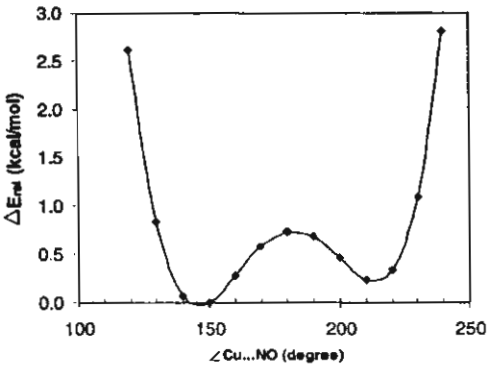

Figure 5. Potential energy curve, relative to the stable NO/Cu−ZSM-5 complex as a function of Cu−NO angle.

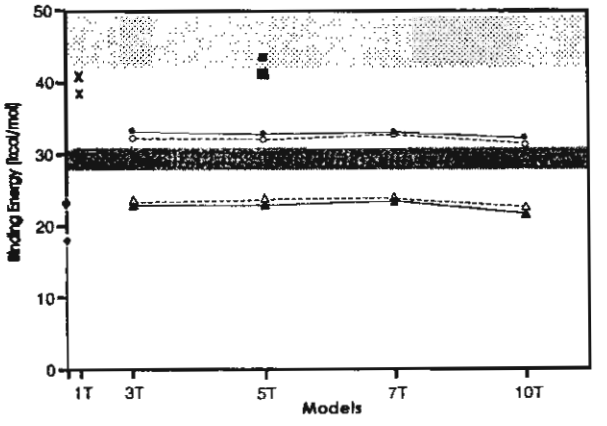

Figure 6. Comparison between calculated and experimental binding energies, for the CO/Cu−ZSM-5 system: the present embedded results (upper solid line), bare cluster results (upper dashed line), experimental range (light shade area, from refs 27 and 51), and previous theoretical predictions (large ◆ from ref 27; large x from ref 46; large ■ from ref 30). For the NO/Cu−ZSM-5 system: the present embedded results (lower solid line), bare cluster results (lower dashed line), experimental range (dark shade area, from ref 18) and previous theoretical predictions (small ◆ from ref 27; small x from ref 46; small ■ from ref 30 and * from ref 79).

Our calculated binding energy of NO to the Cu−ZSM-5, including the BSSE and ZPE corrections, is about 22 kcal/mol. Note that previous calculated binding energies of NO adsorption are very scattered, ranging from 17 to 52 kcal/mol, as shown in Figure 6.[18,29,30,34,44,46,47,78,79] The NO binding energy estimated by Chakraborty et al.[18] from TPD results of Li and Armor is 43.9−49.5 kcal/mol and that estimated from Schay and Guczi's results is 47.6−49.5 kcal/mol. These experimental estimations are much higher than our prediction for the NO binding energy and higher than the experimental CO binding energy as well. However, recent experiments on successive adsorption of CO and NO[15,16] found that CO molecules can displace NO molecules adsorbed on the active site of Cu−ZSM-5. This indicates that the binding energy of NO should be smaller than that of CO and thus supports our results. Note that our relative CO/NO binding energies (32.3/21.8 kcal/mol) are consistent with those from the previous calculations of Schneider et al. (40.9/38.5 kcal/mol)[26] and Brand et al. (24.7/17.0 kcal/mol).[27] Furthermore, the binding energy of NO to Cu−Zeolite-Y was determined to be 20 kcal/mol by IR spectroscopy,[80] and a different absorption experiment also showed that NO can bind to the Cu−ZSM-5 tighter than to the Cu−Zeolite-Y.[53] Due to the fact that Zeolite-Y and ZSM-5 have the same order of pore size, the binding energies of NO to these zeolites should not be too different. Combining all of these experimental facts, the NO binding energy should be slightly larger than 20 kcal/mol and thus fully consistent with our results.

Conclusions

We presented a systematic theoretical study on the structure of the Lewis basic active site of the Cu−ZSM-5 zeolite and the adsorption properties of NO and CO on this zeolite. Both cluster and embedded cluster methodologies were employed to study the effects of the cluster size and of the Madelung potential. From a theoretical point of view, we found that the effects of the cluster size and of the Madelung potential are small in the NO and CO adsorption properties. However, these effects are noticeable in the Cu^+ binding energy. Comparing all models considered in this study ranging from 3T to 10T, the 5T cluster gives the optimal cost per performance ratio and thus provides a more practical model for future studies on this system. For NO and CO adsorption, we found that the zeolite framework plays a significant role in the adsorption mechanism. The calculated adsorption properties, namely, adsorption structure, binding energy, and vibrational frequency of CO on Cu−ZSM-5 zeolite, agree well with available experimental results. Compared to previous studies, the Madelung potential is expected to contribute the correct blue shift of an adsorbed CO and red shift of an adsorbed NO. Particularly, the calculated CO binding energy of 32.3 kcal/mol is in excellent agreement with the available experimental data from 29 to 32 kcal/mol. For NO adsorption, we were able to explain to the difference between our predictions of the bent adsorption structure with the experimentally observed linear structure. The calculated NO binding energy of 21.8 kcal/mol is smaller than the estimated experimental values ranging from 44 to 50 kcal/mol. However, our result is consistent with recent experimental observation that the NO binding energy should be smaller than that of CO and is within the range of NO binding energy in the similarly pore sized Cu−Y zeolite. The calculated red shift in the adsorbed NO stretching frequency also agrees well with experiments.

The study further supports the use of the embedded cluster model to study adsorption in zeolites, particularly metal-exchanged zeolites, and establishes a foundation for future studies of the catalytic activity of Cu−ZSM-5 in reduction of NO_x species.

Acknowledgment. This work is supported in part by the Royal Golden Jubilee Ph.D. project of Thailand, the University of Utah, and the National Science Foundation. The computer support from the Center of High Performance Computing at the University of Utah is gratefully acknowledged.

References and Notes

(1) Iwamoto, M.; Yahiro, H.; Tanda, K.; Mizuno, N.; Mine, Y.; Kagawa, S. *J. Phys. Chem.* **1991**, *95*, 3727.

(2) Sato, S.; Yoshihiro, Y.; Yahiro, H.; Mizuno, N.; Iwamoto, M. *Appl. Catal.* **1991**, *70*, L1.

(3) Shelef, M. *Catal. Lett.* **1992**, *15*, 305.

(4) Li, Y. J.; Armor, J. N. *Appl. Catal.* **1991**, *76*, L1.

(5) Li, Y. J.; Hall, W. K. *J. Catal.* **1991**, *129*, 202.

(6) Armor, J. N. *Catal. Today* **1997**, *38*, 163.

(7) Anpo, M.; Matsuoka, M.; Hanou, K.; Mishima, H.; Yamashita, H.; Patterson, H. H. *Coord. Chem. Rev.* **1998**, *171*, 175.

(8) Lamberti, C.; Salvalaggio, M.; Bordiga, S.; Geobaldo, F.; Spoto, G.; Zecchina, A.; Vlaic, G.; Bellatreccia, M. *J. Phys. IV* **1997**, *7*, 905.

(9) Lamberti, C.; Bordiga, S.; Salvalaggio, M.; Spoto, G.; Zecchina, A.; Geobaldo, F.; Vlaic, G.; Bellatreccia, M. *J. Phys. Chem. B* **1997**, *101*, 344.

(10) Bordiga, S.; Palomino, G. T.; Arduino, D.; Lamberti, C.; Zecchina, A.; Arean, C. O. *J. Mol. Catal. A: Chem.* **1999**, *146*, 97.
(11) Bordiga, S.; Lamberti, C.; Palomino, G. T.; Geobaldo, F.; Arduino, D.; Zecchina, A. *Microporous Mesoporous Meter.* **1999**, *30*, 129.
(12) Dedecek, J.; Wichterlova, B. *Phys. Chem. Chem. Phys.* **1999**, *1*, 629.
(13) Arean, C. O.; Palomino, G. T.; Zecchina, A.; Spoto, G.; Bordiga, S.; Roy, P. *Phys. Chem. Chem. Phys.* **1999**, *1*, 4139.
(14) Arean, C. O.; Tsyganenko, A. A.; Platero, E. E.; Garrone, E.; Zecchina, A. *Angew. Chem., Int. Ed.* **1998**, *37*, 3161.
(15) Borovkov, V. Y.; Jiang, M.; Fu, Y. L. *J. Phys. Chem. B* **1999**, *103*, 5010.
(16) Kuroda, Y.; Kumashiro, R.; Yoshimoto, T.; Nagao, M. *Phys. Chem. Chem. Phys.* **1999**, *1*, 649.
(17) Kuroda, Y.; Mori, T.; Yoshikawa, Y.; Kittaka, S.; Kumashiro, R.; Nagao, M. *Phys. Chem. Chem. Phys.* **1999**, *1*, 3807.
(18) Trout, B. L.; Chakraborty, A. K.; Bell, A. T. *J. Phys. Chem.* **1996**, *100*, 17582.
(19) Liu, D. J.; Robota, H. J. *Catal. Lett.* **1993**, *21*, 291.
(20) Dedecek, J.; Sobalik, Z.; Tvaruzkova, Z.; Kaucky, D.; Wichterlova, B. *J. Phys. Chem.* **1995**, *99*, 16327.
(21) Wichterlova, B.; Dedecek, J.; Vondrova, A. *J. Phys. Chem.* **1995**, *99*, 1065.
(22) Chen, L.; Chen, H. Y.; Lin, J.; Tan, K. L. *Inorg. Chem.* **1998**, *37*, 5294.
(23) Jang, H. J.; Hall, W. K.; Ditri, J. *J. Phys. Chem.* **1996**, *100*, 9416.
(24) Kuroda, Y.; Yoshikawa, Y.; Emura, S.; Kumashiro, R.; Nagao, M. *J. Phys. Chem. B* **1999**, *103*, 2155.
(25) Lamberti, C.; Spoto, G.; Scarano, D.; Paze, C.; Salvalaggio, M.; Bordiga, S.; Zecchina, A.; Palomino, G. T.; Dacapito, F. *Chem. Phys. Lett.* **1997**, *269*, 500.
(26) Schneider, W. F.; Hass, K. C.; Ramprasad, R.; Adams, J. B. *J. Phys. Chem.* **1996**, *100*, 6032.
(27) Brand, H. V.; Redondo, A.; Hay, P. J. *J. Phys. Chem. B* **1997**, *101*, 7691.
(28) Ramprasad, R.; Schneider, W. F.; Hass, K. C.; Adams, J. B. *J. Phys. Chem. B* **1997**, *101*, 1940.
(29) Hass, K. C.; Schneider, W. F. *J. Phys. Chem.* **1996**, *100*, 9292.
(30) Hass, K. C.; Schneider, W. F. *Phys. Chem. Chem. Phys.* **1999**, *1*, 639.
(31) Rice, M. J.; Chakraborty, A. K.; Bell, A. T. *J. Phys. Chem. A* **1998**, *102*, 7498.
(32) Schneider, W. F.; Hass, K. C.; Ramprasad, R.; Adams, J. B. *J. Phys. Chem. B* **1997**, *101*, 4353.
(33) Trout, B. L.; Chakraborty, A. K.; Bell, A. T. *J. Phys. Chem.* **1996**, *100*, 4173.
(34) Yokomichi, Y.; Yamabe, T.; Ohtsuka, H.; Kakumoto, T. *J. Phys. Chem.* **1996**, *100*, 14424.
(35) Zhanpeisov, N. U.; Matsuoka, M.; Mishima, H.; Yamashita, H.; Anpo, M. *THEOCHEM J. Mol. Struct.* **1998**, *454*, 201.
(36) Derouane, E. G.; Fripiat, J. G. *Zeolites* **1985**, *5*, 165.
(37) Alvaradoswaisgood, A. E.; Barr, M. K.; Hay, P. J.; Redondo, A. *J. Phys. Chem.* **1991**, *95*, 10031.
(38) Spoto, G.; Zecchina, A.; Bordiga, S.; Ricchiardi, G.; Martra, G.; Leofanti, G.; Petrini, G. *Appl. Catal., B* **1994**, *3*, 151.
(39) Nachtigallova, D.; Nachtigall, P.; Sierka, M.; Sauer, J. *Phys. Chem. Chem. Phys.* **1999**, *1*, 2019.
(40) Sarkany, J. *J. Mol. Struct.* **1997**, *410*, 145.
(41) Wichterlova, B.; Dedecek, J.; Sobalik, Z.; Vondrova, A.; Klier, K. *J. Catal.* **1997**, *169*, 194.
(42) Aylor, A. W.; Larsen, S. C.; Reimer, J. A.; Bell, A. T. *J. Catal.* **1995**, *157*, 592.
(43) Valyon, J.; Hall, W. K. *J. Catal.* **1993**, *143*, 520.
(44) Kanougi, T.; Tsuruya, H.; Oumi, Y.; Chatterjee, A.; Fahmi, A.; Kubo, M.; Miyamoto, A. *Appl. Surf. Sci.* **1998**, *132*, 561.
(45) Rodriguez-santiago, L.; Sierka, M.; Branchadell, V.; Sodupe, M.; Sauer, J. *J. Am. Chem. Soc.* **1998**, *120*, 1545.
(46) Schneider, W. F.; Hass, K. C.; Ramprasad, R.; Adams, J. B. *J. Phys. Chem. B* **1998**, *102*, 3692.
(47) Kobayashi, H.; Ohkubo, K. *Appl. Surf. Sci.* **1997**, *121*, 111.
(48) Zhanpeisov, N. U.; Nakatsuji, H.; Hada, M.; Nakai, H.; Anpo, M. *Catal. Lett.* **1996**, *42*, 173.
(49) Civalleri, B.; Garrone, E.; Ugliengo, P. *J. Phys. Chem. B* **1998**, *102*, 2373.
(50) Blint, R. J. *J. Phys. Chem.* **1996**, *100*, 19518.
(51) Kumashiro, R.; Kuroda, Y.; Nagao, M. *J. Phys. Chem. B* **1999**, *103*, 89.
(52) Cheung, T.; Bhargava, S. K.; Hobday, M.; Foger, K. *J. Catal.* **1996**, *158*, 301.
(53) Valyon, J.; Hall, W. K. *J. Phys. Chem.* **1993**, *97*, 1204.
(54) Brandle, M. S. Joachim; Dovesi, Roberto; Harrison, Nicholas M. *J. Chem. Phys.* **1998**, *109*, 10379.
(55) Civalleri, B.; Zicovich-Wilson, C. M.; Ugliengo, P.; Saunders, V. R.; Dovesi, R. *Chem. Phys. Lett.* **1998**, *292*, 394.
(56) Hill, J.-R. F.; Clive, M.; Delley, B. *J. Phys. Chem. A* **1999**, *103*, 3772.
(57) Kessi, A.; Delley, B. *Int. J. Quantum Chem.* **1998**, *68*, 135.
(58) Nicholas, J. B.; Hess, A. C. *J. Am. Chem. Soc.* **1994**, *116*, 5428.
(59) Shah, R.; Payne, M. C.; Lee, M. H.; Gale, J. D. *Science* **1996**, *271*, 1395.
(60) Stich, I.; Gale, J. D.; Terakura, K.; Payne, M. C. *J. Am. Chem. Soc.* **1999**, *121*, 3292.
(61) White, J. C.; Nicholas, J. B.; Hess, A. C. *J. Phys. Chem. B* **1997**, *101*, 590.
(62) Sherwood, P.; Devries, A. H.; Collins, S. J.; Greatbanks, S. P.; Burton, N. A.; Vincent, M. A.; Hillier, I. H. *Faraday Discuss.* **1997**, 79.
(63) Greatbanks, S. P.; Hillier, I. H.; Sherwood, P. *J. Comput. Chem.* **1997**, *18*, 562.
(64) Stefanovich, E. V.; Truong, T. N. *J. Phys. Chem. B* **1998**, *102*, 3018.
(65) Vollmer, J. M.; Stefanovich, E. V.; Truong, T. N. *J. Phys. Chem. B* **1999**, *103*, 9415.
(66) Limtrakul, J.; Khongpracha, P.; Jungsuttiwong, S.; Truong, T. N. *J. Mol. Catal. A: Chem.* **2000**, *153*, 155.
(67) Sierka, M.; Sauer, J. *Faraday Discuss.* **1997**, 41.
(68) Sierka, M.; Sauer, J. *J. Mol. Graph Model* **1998**, *16*, 274.
(69) Insight II Release 95.0; BIOSYM/MSI: San Diego, 1995.
(70) Ferrari, A. M.; Neyman, K. M.; Rosch, N. *J. Phys. Chem. B* **1997**, *101*, 9292.
(71) Frisch, M. J.; Trucks, G. W.; H. B. Schlegel, G. E. S.; Robb, M. A.; Cheeseman, J. R.; Zakrzewski, V. G.; Montgomery, J. A.; Stratmann, R. E.; Burant, J. C.; Dapprich, S.; Millam, J. M.; Daniels, A. D.; Kudin, K. N.; Strain, M. C.; Farkas, O.; Tomasi, J.; Barone, V.; Cossi, M.; Cammi, R.; Mennucci, B.; Pomelli, C.; Adamo, C.; Clifford, S.; Ochterski, J.; Petersson, G. A.; Ayala, P. Y.; Cui, Q.; Morokuma, K.; Malick, D. K.; Rabuck, A. D.; Raghavachari, K.; Foresman, J. B.; Cioslowski, J.; Ortiz, J. V.; Stefanov, B. B.; Liu, G.; Liashenko, A.; Piskorz, P.; Komaromi, I.; Gomperts, R.; Martin, R. L.; Fox, D. J.; Keith, T.; Al-Laham, M. A. Peng, C. Y.; Nanayakkara, A.; Gonzalez, C.; Challacombe, M.; Gill, P. M. W.; Johnson, B. G.; Chen, W.; Wong, M. W.; Andres, J. L.; Head-Gordon, M.; Replogle, E. S.; Pople, J. A. *Gaussian 98 (Revision A.7)*; Pittsburgh, PA, 1998.
(72) Yamashita, H.; Matsuoka, M.; Tsuji, K.; Sioya, Y ; Anpo, M.; Che, M. *J. Phys. Chem.* **1996**, *100*, 397.
(73) Yamashita, H.; Matsuoka, M.; Anpo, M.; Che, M. *J. Phys IV* **1997**, *7*, 941.
(74) Sengupta, D.; Schneider, W. F.; Hass, K. C.; Adams, J. B. *Catal. Lett.* **1999**, *61*, 179.
(75) Scarano, D.; Bordiga, S.; Lamberti, C.; Spoto, G.; Ricchiardi, G.; Zecchina, A.; Arean, C. O. *Surf. Sci.* **1998**, *411*, 272.
(76) Aylor, A. W. L.; Sarah, C.; Reimer, J. A.; Bell, A. T. *J. Catal.* **1995**, *157*, 592.
(77) Giamello, E.; D, M.; Magnacca, G.; Morterra, C.; Shioya, Y.; Nomura, T.; Anpo, M. *J. Catal.* **1992**, *136*, 510.
(78) Brand, H. V.; Redondo, A.; Hay, P. J. *J. Mol. Catal. A: Chem.* **1997**, *121*, 45.
(79) Tajima, N.; Hashimoto, M.; Toyama, F.; Elnahas, A. M.; Hirao, K. *Phys. Chem. Chem. Phys.* **1999**, *1*, 3823.
(80) Davydov, A. A. *Zh. Fiz. Khim.* **1991**, *65*, 269.

ELSEVIER Studies in Surface Science and Catalysis, 135 (2001) 2518

A theoretical study of adsorption of carbon monoxide on Ag-ZSM-5 zeolite

*Siriporn Jungsuttiwong [(a)], P. Khongpracha [(a)], T. N. Truong [(b)], and Jumras Limtrakul [(a)]**

[a] *Laboratory for Computational & Applied Chemistry, Chemistry Department, Kasetsart University, Bangkok 10900, THAILAND; e-mail: fscijrl@ku.ac.th*
[b] *Henry Eyring Center for Theoretical Chemistry, Department of Chemistry, University of Utah, 315 S 1400 E, rm 2020, Salt Lake City, UT 84112, USA*

Adsorption of carbonmonoxide on the silver ion-exchanged Ag-ZSM-5 zeolite has been studied using both quantum cluster and embedded cluster at the models B3LYP/6-31G(d,p) level of theory. The Ag^+...Oz distance in Ag^+-ZSM-5 complexes is predicted to be 2.26 Å for the quantum cluster and 2.32 Å for the embedded cluster, the latter is in agreement with the experimental value of 2.30 ± 0.03 Å. The optimized Ag^+...CO distances in the Ag^+-ZSM-5 are evaluated to be 2.04 and 2.07 Å for quantum and embedded clusters, respectively. The corresponding CO stretching mode in the Ag^+-ZSM-5/CO is calculated to be 2157 cm^{-1} for the quantum cluster and shifted to 2171 cm^{-1} when the zeolite lattice framework is taken into account ,which is close to the observed values by FITR (2190-2192 cm^{-1}). Similar trends were observed for the Cu^+-ZSM-5/CO complexes: Cu^+-Oz = 2.00 (2.00 ± 0.02) Å , Cu^+-CO = 1.85 (1.89) Å , ΔE_{ads} = -33.56 (-28.7) kcal/mol; values in parentheses are those obtained from experimental results. For the Ag^+-ZSM-5/CO complex, ΔE_{ads} amounts to 60% of the adsorption energy value for the Cu^+-ZSM-5/CO complex which is due to the lengthened Ag^+...CO distance as compared to the Cu^+...CO distance in the Cu^+-complex. The results obtained for the Ag^+-ZSM-5 complex indicates that correction of the long-range electrostatic potential of the zeolitic crystal in the quantum cluster is found to yield reliable results when compared to the experiment observation.

1. INTRODUCTION

The transition-metal cation-exchanged zeolites are found to be effective catalysts in many industrially important processes [1-16]. Ag^+-exchanged zeolite has attracted interest for several catalytic and photocatalytic processes such as photochemical dissociation of H_2O into H_2 and O_2 [17-18], the disproportion of ethylbenzene [19], the selective reduction of NO by ethylene [20] and the photocatalytic decomposition of NO [21-26].

The adsorption CO on the Ag^+-exchanged zeolites has been recently investigated by Bordiga et al [27]. However, the structure, bonding, and energetics of these transition-metal-exchanged zeolites and their interactions with probe molecules are not well understood, and this hinders understanding of many of the above-mentioned processes. To the best of our knowledge, no theoretical works on Ag^+-ZSM-5/CO complexes are reported. In this study, the density functional theory method has been employed to compare the local active sites of

the Ag^+-ZSM-5 and Cu^+-ZSM-5 complexes and to investigate the CO adsorption on these catalysts. Attempts have been made to make correction for the long-range electrostatic potential of zeolite in cluster calculations by employing embedded approaches [28-40]. We have demonstrated that the ab initio embedded cluster method can be exploited to provide reliable results when compared to the experiment observation [28-29].

2. METHOD

The bare quantum clusters are selected to model specifically to Ag-ZSM-5 zeolite. In the MFI framework models, the dangling bonds of Si atoms are capped by hydrogen atoms at the boundary, while the Si–H bonds are fixed along with the corresponding Si–O bonds of the framework [41].

In the embedded cluster approach, the electrostatic Madelung potential, corresponding to zeolite framework outside of the quantum cluster, was represented by partial point charges located at the zeolitic lattice point. Using an approach recently employed by us [28-29, 40], charges close to the quantum cluster were treated explicitly while the remaining infinite lattice Madelung potential was represented by a set of surface charges that were evaluated from the surface charge representation of the external electrostatic potential (SCREEP) method.

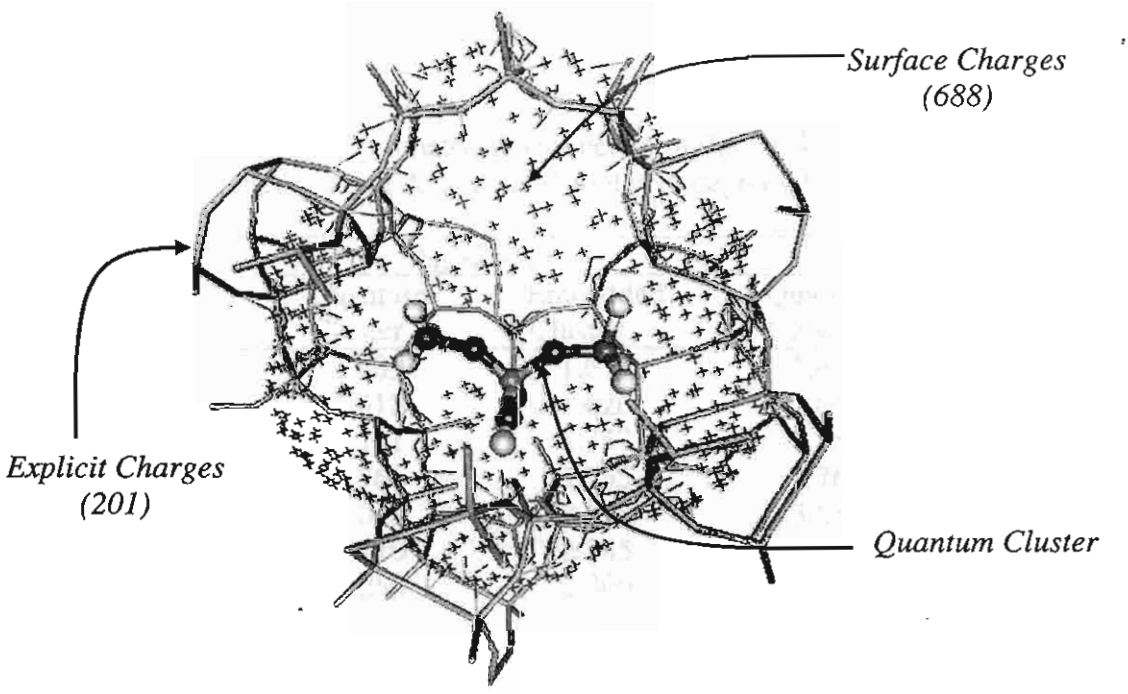

Fig.1 The cluster $H_3SiOHAl(OH)_2OSiH_3$ in the ZSM-5 framework structure.

In this present work, the total Madelung potential is represented by 201 explicit charges and 688 surface charges. More details on this method can be found elsewhere [40]. Due to the small number of point charges, additional computational consumption is often less than 5% compared to bare cluster calculations.

Geometry optimizations were investigated with the density functional theory at the B3LYP/6-31G(d,p) level of theory using the GAUSSIAN 94 [42] program code. The basis sets employed for transition metal potentials were of Hay-Wadt effective core potential type [43-45]. The computations were carried out using an IBM SP2 computer at KU Computing Center and a DEC Alphastation 250 and HP 9000/700 workstation at the Laboratory for Computational and Applied Chemistry (LCAC) at Kasetsart University.

3. RESULTS AND DISCUSSION

The effect of metal ions on the structure and bonding of zeolitic catalysts is investigated at cluster and embedded cluster approaches. The fully optimized geometry structures for Ag^{+}-ZSM-5 zeolite and the interaction with CO molecules are documented in Table 1.

3.1 Cationic environment: Ag^{+}-ZSM-5

Cluster and embedded cluster models for Ag^{+}-ZSM5 zeolite are shown in Fig.2. The transition metal ions do not bind with a particular bridging oxygen atom in the $[AlO_4]^{-}$, but symmetrically bidentated to the O1 and O2 of the $[AlO_4]^{-}$ tetrahedron and the interaction has ionic character. Table 1 indicates that the charge compensating metal ions can affect the ≡Si-O-Al≡ by weakening the Si-O and Al-O bonds as compared to the anionic framework. Comparing the result between cluster and embedded cluster models of Ag^{+}-ZSM5 complexes, we found the Al-O1 and Al-O2 distances are shortened by 0.0034 and 0.0113 Å, respectively (Al-O1 = 1.761 Å vs. 1.757 Å and Al-O2 =1.766 Å vs. 1.755 Å).

Table 1
B3LYP/6-31G (d,p) optimized geometrical parameters of the Ag^{+}-ZSM5 and Ag^{+}-ZSM5 /CO systems. (Bond lengths are in Å. and bond angles in degrees.)

Bond or angle	Ag^{+}-ZSM5		Ag^{+}-ZSM5 /CO	
	Quantum Cluster	Embedded Cluster	Quantum Cluster	Embedded Cluster
$Si_1 - O_1$	1.609	1.615	1.638	1.618
$Si_2 - O_2$	1.612	1.626	1.643	1.629
$Al - O_1$	1.761	1.757	1.759	1.756
$Al - O_2$	1.766	1.755	1.765	1.754
Al---Ag	3.048	3.108	3.055	3.103
$O_1 - Ag$	2.270	2.345	2.251	2.324
$O_2 - Ag$	2.250	2.300	2.237	2.277
C – O	-	-	1.135	1.134
Ag---C	-	-	2.038	2.069
Ag – C – O	-	-	179.1	176.4
$O_1 - Ag - O_2$	69.6	67.6	69.4	67.9
$O_1 - Al - O_2$	94.0	94.7	92.9	94.1
$Ag - O_2 - O_1 - Al$	191.2	169.2	185.8	175.6
q (Ag^{+})	0.5165	0.6041	0.4511	0.5113
ν(CO) (cm^{-1})	-	-	2157.6	2171.1

The calculated metal...O distances increase when the zeolitic lattice framework is included (Ag^+...O1 = 2.270 Å vs. 2.345 Å and Ag^+...O2 = 2.250 Å vs. 2.301 Å). The Ag^+...Al distance is also lengthened by 0.060 Å, indicating that a weakening of the attachment of the metal cation to zeolite framework.

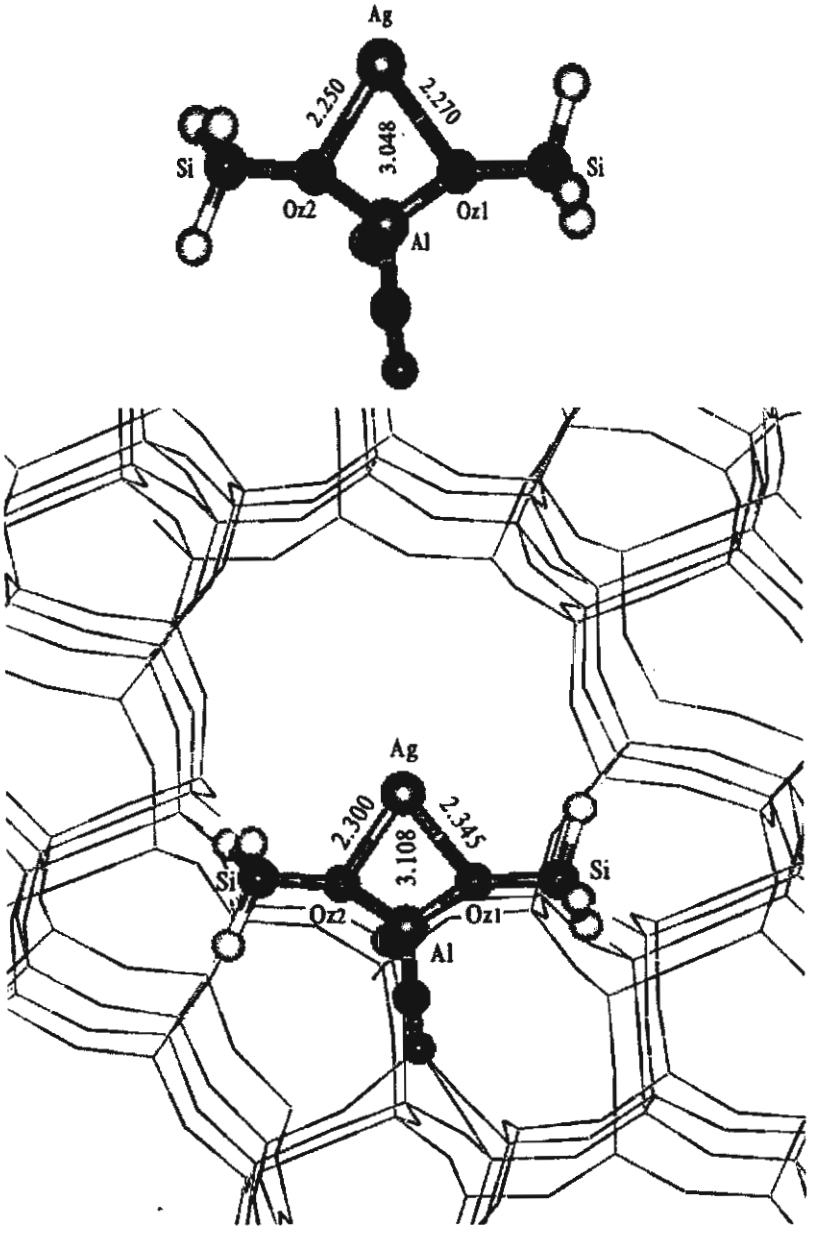

Fig. 2 Cluster and embedded cluster models of the Ag-ZSM-5 zeolite. All values given in angstroms.

Further support for the reliability of using the embedded cluster model is confirmed by the results of EXAFS measurement [27]: the Ag^+...O of the Ag^+-ZSM5 complex has been estimated to be 2.30 $\pm$ 0.03 Å, whereas our computed distance is 2.32 Å .

Similar trends taken from the cluster and embedded models are also observed for the Cu^+-ZSM5 zeolites. The Al-O1 and Al-O2 distances are shortened by 0.0037 and 0.0104 Å, respectively (Al-O1 = 1.769 vs. 1.765 Å and Al-O2 = 1.773 vs. 1.763 Å).

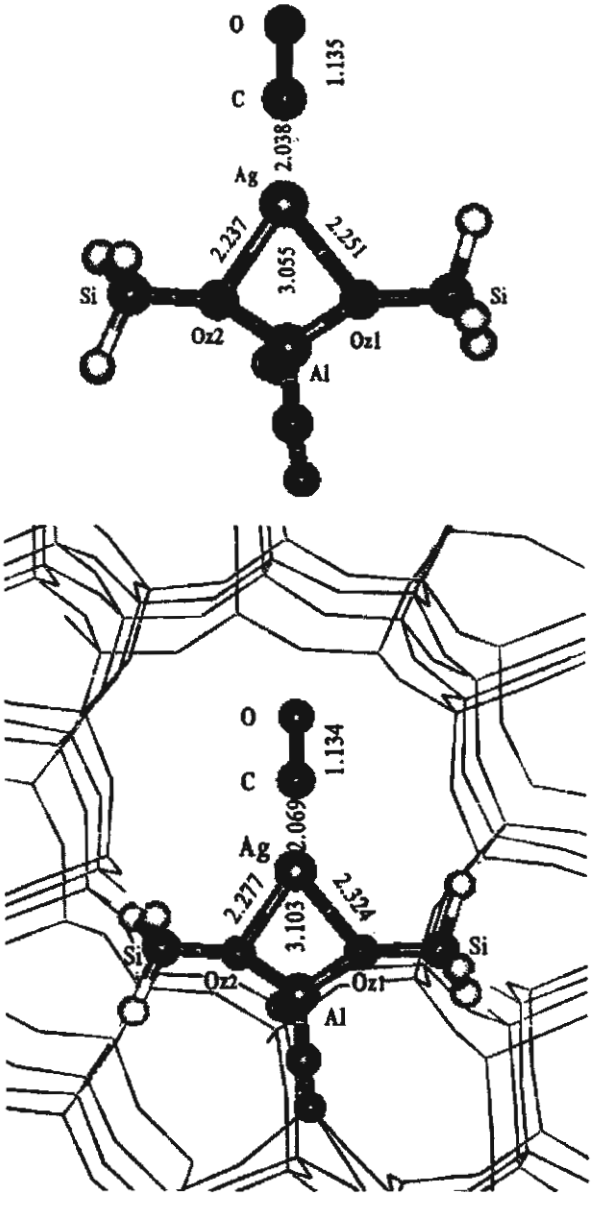

Fig.3 Cluster and embedded cluster models of the Ag-ZSM-5/CO complex. All values given in angstroms.

The metal...O distances increase when the zeolitic lattice framework is included (Cu^+...O1 = 2.007 Å vs. 2.062 Å and Cu ...O2 = 1.996 Å vs. 2.029 Å) and the Cu^+...Al distance is lengthened by 0.039 Å (2.757 vs. 2.796 Å). These values are larger than those derived previously by Trout et al. [46] based on the density functional theory with local spin density approximation (DFT/LSDA) results using the uncontracted Huzinaga basis set (Cu^+···O1 = 2.0 Å, Cu^+···O2 = 1.9 Å and Cu^+···Al = 2.4 Å). These small differences can be attributed to the

overbinding at this DFT/LSDA level as already noted by Bell et al. [47]. Comparison can also be made with HF/6-31G** level of theory obtained by Blint [48]. The two $Cu^{+}\cdots O_z$ distances are estimated to be 2.14 Å. Our predicted $Cu^{+}\cdots Oz$ value of 2.04 Å is in close agreement with the results of DFT reported by Rice et al. [47] ($Cu^{+}\cdots O_{z1}$ = 2.06 Å, $Cu^{+}\cdots O_{z2}$ = 1.95 Å and $Cu^{+}\cdots Al$ = 2.64 Å) and experimental EXAFS technique reported by Lamberti et al. [49] (the average $Cu^{+}\cdots O_z$ bond length is 2.00 ± 0.02 Å). The results obtained for the Ag^{+}-ZSM-5 and Cu^{+}-ZSM-5 complexes clearly indicate that correction of quantum cluster by including zeolite lattice crystal is found to yield reliable data when compared to the experiment observation [28-29].

3.2 Adsorption of CO on Ag^{+}-ZSM-5

Cluster and embedded cluster models for interaction of CO with Ag^{+}-ZSM-5 zeolite are shown in Fig. 3. Selected geometrical parameters and their binding energies (bases set superposition errors are included) are documented in Table 1. We found that adsorption of CO does not affect the zeolite framework significantly. The geometry of the Ag^{+}-ZSM-5 active site changes by at most 0.002 Å for bond distances and 1° for angles due to CO adsorption. This result has an important implication that is, in future theoretical studies of adsorption of similar species, it is possible, without loosing much accuracy, to constrain the zeolite framework in optimization of the complex structure. This would accelerate the convergence and reduce significantly the computational cost.

The distances between the Ag^{+} ion and the C atom of the CO molecule were evaluated to be 2.04 and 2.07 Å for the quantum cluster and embedded cluster models, respectively. Our predicted metal...CO distances are in good agreement with the observed experimental values ($Ag^{+}...CO_z$ = 2.07 vs. 2.10 Å). The adsorption energy (ΔE_{ads}) of the Ag^{+}-ZSM-5/CO complex amounts to 60% of the ΔE_{ads} value for the Cu^{+}-ZSM-5/CO complex (ΔE_{ads} (Ag^{+}-ZSM-5/CO) = –20.29 kcal/mol ; ΔE_{ads}(Cu^{+}-ZSM-5/CO) = –33.56 kcal/mol).

The C-O stretching mode of CO adsorbed on the Ag^{+}-ZSM-5 and Cu^{+}-ZSM-5 are 2159 and 2171 cm^{-1}, respectively. The calculated high frequency of C-O stretching in the $Ag^{+}...CO$ complex is fully in agreement with the experimental findings of Zecchina et.al. [27] as only σ-donation is dominated, not the π-contribution. This is due in part to the large $Ag^{+}...C$ distance prohibiting π-back bonding in silver carbonyls [50] which was confirmed.

4. CONCLUSIONS

Calculated results obtained from the embedded cluster method at B3LYP/6-31G(d,p) yielded a metal-oxygen distance of 2.300 (2.30±0.03) Å for the Ag^{+}-ZSM-5; the value in the parenthesis is taken from the experimental results. The Madelung potential, represented by sets of point charges surrounding the quantum cluster causes metal-oxygen distances to be elongated by 0.05-0.07 Å which make all predicted results agree very well with the observations. The observed differences in the metal-O distances assigned to the larger ionic radius of the Ag^{+} ion, as compared to the Cu^{+}. The corresponding adsorption energies were found to be –33.56 (28.7) and –20.29 and kcal/mol for their interaction with CO molecules, respectively, The C-O stretching modes of CO adsorbed on the Cu^{+}-ZSM-5 and Ag^{+}-ZSM-5 are 2159 and 2171 cm-1, respectively. The calculated high frequency of C-O stretching in the Ag^{+}-ZSM-5 complex is on account of the larger Ag^{+}-C bond (2.07 Å) as compared to the

Cu^+-C bond (1.85 Å). This large distance can to some extent prevent the contribution of the π-back bonding in silver carbonyl complexes.

ACKNOWLEDGEMENTS

This work was supported by grants from the Thailand Research Fund (TRF) for supporting the research career development project (The TRF-research scholar) and the Royal Golden Jubilee Ph.D. Programme to P.K. and S.J., as well as the Kasetsart University Research and Development Institute (KURDI). Our sincere thanks are due to Professors R. Ahlrichs (Karlsruhe, Germany) for his continued support of this work.

REFERENCES

[1] M. Iwamoto, S. Yoke, K. Sakai and S. Kagawa, J. Chem. Soc. Faraday Trans., 77 (1981) 1629.
[2] M. Iwamoto, H. Furukawa, Y. Mine, F. Uemura, S. Mikuriya and S. Kagawa, J. Chem. Soc., Chem. Commun., (1986) 1272.
[3] M. Iwamoto and H. Yahiro, Catal. Today, 22 (1994) 5.
[4] M. Iwamoto, H. Furukawa and S. Kagawa, in: Y. Murukama, A. Ichijima, J.W. Ward (Eds.), New Developments in Zeolite Science and Technology, Elsevier, Amsterdam, 1986, p 943.
[5] M. Iwamoto and H. Hamada, Catal. Today, 10 (1991) 57.
[6] M. Iwamoto, H. Yahiro, K. Tanada, Y. Mozino, Y. Mine and S. Kagawa, J. Phys. Chem., 95 (1991) 3727.
[7] Y. Li and J.N. Armor, Appl. Catal. B, 1 (1992) L31.
[8] Y. Teraoka, H. Ogawa, H. Furukawa and S. Kagawa, Catal. Lett., 12 (1992) 361.
[9] Y. Li, P.J. Battavio and J.N. Armor, J. Catal., 142 (1993) 561.
[10] K.C.C. Kharas, Appl. Catal. B, 2 (1993) 207.
[11] Y. Zhang, M. Flytzani-Stephanopoulos, in: J. N. Armor (Ed.), Catalytic Decomposition of Nitric Oxide over Promoted Copper-Ion-Exchanged ZSM-5 Zeolites. In Environmental Catalysis, ACS Symposium Series 552, American Chemical Society: Washington, DC, 1994, p 7.
[12] G. Centi, C. Nigro, S. Perathoner and G. Stella, in: J. N. Armor (Ed.), Reactivity of Cu-Based Zeolites and Oxides in the Conversion of NO in the Presence or Absence of O_2. In Environmental Catalysis, ACS Symposium Series 552, American Chemical Society, Washington, DC, 1994, p 22.
[13] A.W. Aylor, S.C. Larsen, J.A. Reimer and A.T. Bell, J. Catal. 157 (1995) 592.
[14] M. Shelef, Chem. Rev., 95 (1995) 209.
[15] M.C. Campa, S. De Rossi, G. Ferraris and V. Indovina, Appl. Catal. B, 8 (1996) 315.
[16] L.J. Lobree, A.W. Aylor, J.A. Reimer and A.T. Bell, J. Catal., 169 (1997) 188.
[17] P.A. Jacobs and J.B. Uytterhoeven, H.K. Beyer, J. Chem. Soc. Chem. Commun., (1997) 128.
[18] G. Calzaferri, S. Hug, T. Hugentobler and B. Sulzberger, J. Photochem., 26 (1984) 109.
[19] T. Baba and Y. Ono, Zeolites, 7 (1987) 292.
[20] S. Sato, Y. Yu-u, H. Yahiro, N. Mizuno and M. Iwamoto, Appl. Catal., 70 (1991) L1.

[21] M. Matsuoka, E. Matsuda, K. Tsuji, H. Yamashita and M. Anpo, Chem. Lett., (1995) 375.
[22] M. Matsuoka, E. Matsuda, K. Tsuji, H. Yamashita and M. Anpo, J. Mol. Catal. A, 107 (1996) 399.
[23] K. Masuda, K. Tsujimura, K. Shinoda and T. Kato, Appl. Catal. B, 8 (1996) 33.
[24] M. Anpo, M. Matsuoka and H. Yamashita, Catal. Today, 35 (1997) 177.
[25] M. Anpo, G.Z. Shu, H. Mishima, M. Matsuoka and H.Yamashita, Catal. Today, 39 (1997) 159.
[26] M. Flytzani-Stephanopoulos and Z. Li, Appl. Catal. A, 165 (1997) 15.
[27] S. Bordiga, G.Turnes Palomino, D. Arduino, C. Lamberti, A. Zecchina and C.O. Arean, J. Mol. Catal. A ,146 (1999) 97.
[28] J. Limtrakul, S. Jungsuttiwong and P. Khongpracha, J. Mol. Struct., 525 (2000) 153.
[29] J. Limtrakul, P. Khongpracha, S. Jungsuttiwong and T.N. Truong, J. Mol. Catal. A, 153 (2000) 155.
[30] R. Vetrivel, C.R.A. Catlow and E.A. Colbourn, Proc. R. Soc. London A, 417 (1988) 81.
[31] M. Allavena, K. Seiti, E. Kassab, Gy. Ferenczy and J.G. Angyan, Chem. Phys. Lett., 168 (1990) 416.
[32] G. Aloisi, P. Barnes, C. R. A. Catlow, R.A. Jackson and A. J. Richards, J. Phys. Chem., 93 (1990) 3573.
[33] J. C. White and A.C. Hess, J. Phys. Chem., 97 (1993) 8703.
[34] E.H. Teunissen, A.J. Jansen, R.A. van Santen and R. Orlando, J. Chem. Phys., 101 (1994) 5865.
[35] A. Kyrlidis, S.J. Cook, A.K. Chakrabory, A.T. Bell and D.N. Theodorou, Phys. Chem., 99 (1995) 1505.
[36] E.H. Teunissen, A. P. J. Jansen and R. A. van Santen, J. Phys. Chem., 99 (1995) 1873.
[37] U. Eichler, M. Brandle and J. Sauer, J. Phys. Chem. B., 101 (1997) 10035.
[38] M. Brandle and J. Sauer, J. Am. Chem. Soc., 120 (1998) 1556.
[39] S.P. Greatbanks, I.H. Hillier, N.A. Burton and P. Sherwood, J. Chem. Phys., 105 (1996) 3370.
[40] E.V. Stefanovich and T.N. Truong, J. Phys. Chem. B, 102 (1998) 3018.
[41] H. van Koningsveld, H. Van Bekkum and J.C. Jansen, Acta Crystallogr. B, 43 (1987) 127.
[42] M.J. Frisch, G.W. Trucks, H.B. Schlegel, P.M.W. Gill, B.G. Johnson, M.W. Wong, J.B. Foresman, M.A. Robb, M. Head-Gordon, E.S. Replogle, R. Gomperts, J.L. Andres, K. Raghavachari, I.S. Binkley, C. Gonzalez, R.L. Martin, D.J. Fox, D.J. DeFrees, J. Baker, J.J.P. Stewart, J.A. Pople, Gaussian 94, Gaussian, Pittsburgh, 1994.
[43] P.J. Hay and W.R. Wadt, J. Chem. Phys., 82 (1985) 270.
[44] W.R. Wadt and P.J. Hay, J. Chem. Phys., 82 (1985) 284.
[45] P.J. Hay and W.R. Wadt, J. Chem. Phys., 82 (1985) 299.
[46] B.L. Trout, A.K. Chakraborty and A.T. Bell, J. Phys. Chem., 100 (1996) 4173.
[47] M.J. Rice, A.K. Chakraborty and A.T. Bell, J. Phys. Chem. A, 102 (1998) 7498.
[48] R.J. Blint, J. Phys. Chem., 100 (1996) 19518.
[49] C. Lamberti, S. Bordiga, M. Salvalaggio, G. Spoto, A. Zecchina, F. Geobaldo, G. Vlaic and M. Bellatreccia, J. Phys. Chem. B, 101 (1997) 344.
[50] P.K. Hurlburt, J.J. Rack, J.S. Luck, S.F. Dec, J.D. Webb, O.P. Anderson and S.H. Strass, J. Am. Chem. Soc., 116 (1994) 10003.

ELSEVIER

Journal of Molecular Catalysis A: Chemical 153 (2000) 155–163

JOURNAL OF MOLECULAR CATALYSIS A: CHEMICAL

www.elsevier.com/locate/molcata

Adsorption of carbon monoxide in H-ZSM-5 and Li-ZSM-5 zeolites: an embedded ab initio cluster study

Jumras Limtrakul [a], Pipat Khongpracha, Siriporn Jungsuttiwong, Thanh N. Truong [b,*]

[a] *Laboratory for Computational and Applied Chemistry, Chemistry Department, Faculty of Science, Kasetsart University, Bangkok 10900, Thailand*

[b] *Henry Eyring Center for Theoretical Chemistry, Department of Chemistry, University of Utah, 315 S 1400 E Rm Dock, Salt Lake City, UT 84112, USA*

Received 7 June 1999; accepted 26 August 1999

Abstract

The absorption of carbon monoxide with H-ZSM-5 and metal-substituted Li-ZSM-5 zeolites has been investigated by using both cluster and embedded cluster approaches at the HF/6–31G(d,p) level of theory. For the H-ZSM-5 zeolite, the binding energy of CO on a 3T quantum cluster is predicted to be 2.25 kcal/mol for the C-bound complex. The O-bound complex was found to be less stable by about 0.84 kcal/mol. Inclusion of the Madelung potential was found to increase the acidity of the Brønsted acidic site and the CO-binding energy to 4.95 kcal/mol, consequently, it leads better agreement with experimental observation. Similar results were also obtained for the Li-ZSM-5/CO complex. The Madelung potential field from the zeolite framework was found to reverse the order of relative stability of C-bound and O-bound adducts in comparison to the Li^+–CO system.

1. Introduction

Zeolite catalysis is of prime importance in many industrial processes due to the size- and shape-selectivity of zeolite crystals and their Brønsted acid sites [1–19]. Recently, metal-substituted zeolites were found to be potential catalysts for decomposition of NO_X and CO from automotive emission and power plants [20–22]. CO adsorption is also used as a probe of the cation loading in ion-exchange processes in zeolites [21]. For this reason, numerous theoretical and experimental studies have been performed to examine the interaction of CO with zeolites [23–36]. To the best of our knowledge, theoretical studies to date are based on small quantum clusters as models of the zeolite Brønsted acid site. Such cluster models sometime can give reasonable estimates of adsorption energy. However, such results does not correspond to any specific zeolite but rather to a generic tetrahedral subunit containing the Brønsted acid site in an unconstrained environment. Recent studies have shown that the Madelung potential is im-

* Corresponding author. Fax: +1-801-581-8433.
E-mail address: truong@mercury.chem.utah.edu (T.N. Truong).

1381-1169/00/$ - see front matter
PII: S1381-1169(99)00339-8

portant in studying adsorption processes due to its long-range electrostatic nature [37,38].

To include the effects of the zeolite framework on the adsorption of CO in zeolites, a periodic electronic structure method can be utilized [39–41]. This corresponds to the high loading case and is often computationally expensive for most zeolites due to their relatively large unit cells. Alternatively, the embedded cluster approach provides a more practical methodology with a little additional computational cost comparing to the bare cluster calculations [37].

In this study, we examine the interaction of CO in both H-ZSM-5 and Li-ZSM-5 zeolites. Particularly, we focus our attention on the importance of the Madelung potential in the structure and energetics of CO adsorption in these zeolites.

2. Computational method and physical models

Cluster and embedded cluster models were used to determine structure and energetics of species in H-ZSM-5 and Li-ZSM-5 zeolites. The quantum cluster in both models consists of three tetrahedral sites including the Brønsted site with capped hydrogen atoms at the boundary, i.e., $H_3SiO(X)Al(OH)_2OSiH_3$ where X is either H or Li atom. The Si–H bonds are fixed

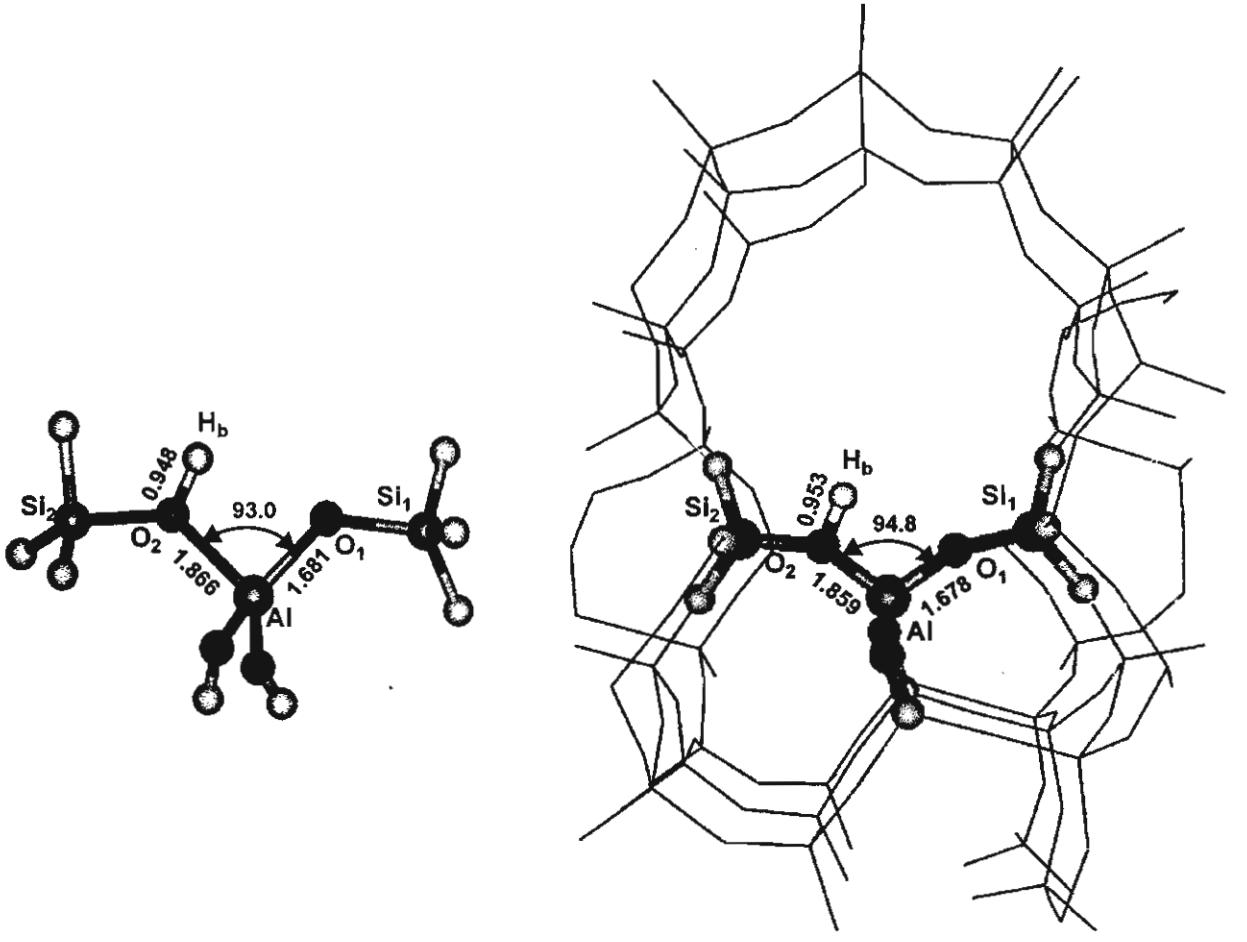

Fig. 1. Cluster and embedded cluster models of the H-ZSM-5 zeolite. Bond distances given in the figures are in Å.